SUPRAMOLECULAR ASSEMBLY OF NEUTRAL AND IONIC DISCOTIC LIQUID CRYSTAL MOLECULES AT INTERFACES

A Thesis
Presented to
The Academic Faculty

By

Prakhar Verma

In Partial fulfilment
of the Requirement for the Degree of
Master of Technology

In

Nanoscience and Technology

INDIAN INSTITUTE OF TECHNOLOGY PATNA

July 2018

Dedicated to my Mom

Acknowledgements

In pursuing this research work, first and foremost, I would like to thank my supervisor **Dr. Alpana Nayak** for her kind support and motivation. Without her valuable guidance and motivation it wouldn't have been possible to complete this research work in the given time frame. I appreciate all her contribution in form of ideas and suggestions to make my master's research work productive and stimulating. I am thankful to her for motivating me to learn molecular dynamics simulations along with the experimental techniques. I thank her for providing me the opportunity to work on fascinating materials and characterization techniques.

I would also like to thank my co-supervisor **Dr. Snehasis Daschakraborty** who helped me learning Molecular Dynamics and Density Functional Theory calculations from the root. He has been the guiding force behind all theoretical modelling and calculations. I would like to express my sincere thanks to him for providing the necessary computational environment under Dept. of Chemistry, IIT Patna and introducing me to cluster computing.

I would like to thank Samapika Mallik for helping me prepare samples and performing characterization on them. I would also like to thank Vikas Dubey for discussing various topics related to MD simulations.

At last, I would like to thank my family and friends for their constant support and belief in me. They have been a source of encouragement throughout my life and in all my pursuits.

Prakhar Verma

Certificate of Approval

This is to certify that the thesis entitled **Supramolecular Assembly of Neutral And Ionic Discotic Liquid Crystal Molecules at Interfaces**, submitted by **PRAKHAR VERMA** to Indian Institute of Technology Patna, for the award of the degree of Master of Technology has been accepted by examination committee and that the student has successfully defended the thesis in the viva-voce examination held today.

Supervisor: ______________________ Date: __________

Co-Supervisor: ______________________ Date: __________

Internal Examiner: ______________________ Date: __________

______________________ __________

External Examiner: ______________________ Date: __________

Certificate

This is to certify that the thesis entitled **Supramolecular Assembly of Neutral And Ionic Discotic Liquid Crystal Molecules at Interfaces**, submitted by **PRAKHAR VERMA** to Indian Institute of Technology Patna, is a record of bona fide research work under my supervision and I consider it worthy of consideration for the degree of Master of Technology of this institute. This work or a part has not been submitted to any university/institution for the award of degree/diploma. The thesis is free from plagiarized material.

Supervisor
Dr. Alpana Nayak
Dept. of Physics
Indian Institute od Technology Patna
Date:

Co-Supervisor
Dr. Snehasis Daschakraborty
Dept. of Chemistry
Indian Institute of Technology Patna
Date:

Declaration of Authorship

I, PRAKHAR VERMA, declare that this thesis titled, 'SUPRAMOLECULAR ASSEMBLY OF NEUTRAL AND IONIC DISCOTIC LIQUID CRYSTAL MOLECULES AT INTERFACES' and the work presented in it are my own. I confirm that:

- This work was done wholly or mainly while in candidature for the award of master's degree at Indian Institute of Technology Patna.
- This thesis or any part of this thesis has not been submitted previously at any university/institution for a degree or any other qualification.
- I have either consulted or acknowledged the published work of others and have clearly mentioned them in this thesis.
- The work that I have quoted from the works of other have always been given credit. With the exception of such quotations, this thesis is entirely my own work.
- I have acknowledged all main sources of help.
- The thesis is based on work done by myself under the guidance of my supervisors and is free from any plagiarized material.

Signed:

Date:

“Things that hurts, instructs”

Benjamin Fanklin

Contents

List of Figures

List of Tables

Abbreviations

ImTp	**I**midazolium **T**riphenylene
DLC	**D**iscotic **L**iquid **C**rystal
HMDS	**H**exa**m**ethyl**d**i**s**ilazane
LB	**L**angmuir **B**lodgett
ESP	**E**quilibrium **S**preading **P**ressure
SPM	**S**canning **P**robe **M**icroscopy
STM	**S**canning **T**unneling **M**icroscopy
AFM	**A**tomic **F**orce **M**icroscopy
DFT	**D**ensity **F**unctional **T**heory
MD	**M**olecular **D**ynamics
SPE	**S**ingle **P**oint **E**nergy
OPLS	**O**ptimized **P**otentials for **L**iquid **S**imulations
SPC/E	**E**xtended / **S**imple **P**oint **C**harge
I-V	**C**urrent **V**oltage **C**haracteristics

Physical Constants

Speed of Light $c = 2.997\ 924\ 58 \times 10^{8}\ \mathrm{ms}^{-1}$

Planck Constant $h = 6.626\ 070\ 04 \times 10^{-34}\ \mathrm{m}^{2}\mathrm{kgs}^{-1}$

Boltzmann Constant $K_B = 1.380\ 648\ 52 \times 10^{-23}\ \mathrm{m}^{2}\mathrm{kgs}^{-2}\mathrm{K}^{-1}$

Avogadro's Number $A_v = 6.022\ 140\ 85 \times 10^{23}$

Symbols

π	Surface Pressure
τ	Transfer Ratio
A_m	Area per molecule
$A_\circ$	Limiting Area per molecule
$\mid E \mid$	Compressional Elastic Modulus
ϵ	Potential Well Depth
σ	Distance at Zero Potential
Δ	Deflection along Z axis
K_x	Stiffness of Cantilever
I	Moment of Inertia

Abstract

Recent studies have shown that Discotic Liquid Crystal (DLC) Molecules can self-assemble and show charge and energy transport properties. The dominant pi-stacking present among these molecules offers a better flow of charge. The flow of charge is dependent upon the separation of two stacked cores. This phenomenon is of great importance for tailoring new generation semiconductor devices. In this research work, the supramolecular organization of neutral and ionic Imidazolium Triphenylene (ImTp) molecule in gas and water surface is studied theoretically and on silicon and silver substrates experimentally. The theoretical investigation was carried out in gas phase using DFT calculations and on surface of water using Molecular Dynamics simulations. The experimental research work includes surface manometry, Langmuir-Blodgett film deposition and morphology of films using atomic force microscopy.

The self-assembly of these discotic molecules is dependent on various parameters such as surface concentration, temperature gradient, electrostatic repulsion, irradiation with polarized light and doping. These materials can be tuned using these properties and are of vital importance for device fabrication. These materials are potential components for photovoltaic, light emitting diode, Lithium ion battery and one dimensional conductor. In recent times, resistive switching memory devices have been attracting lots of attention round the globe. Researchers have been investigating wide range of organic and inorganic materials to find out the most appropriate one for successful device applications. Notably, DLCs, which are potential candidates for resistive switching operations, have not yet been explored. This thesis deals with understanding the supramolecular organization of neutral and ionic ImTp DLC molecules. Such studies are expected to play an important role in designing not only the resistive switching devices but also other kinds of devices as per their specific needs.

Chapter 1

Introduction

The notion of state of matter that can flow like liquid but has crystal like orientation is termed as Liquid Crystal. The intermediate state of matter between solid and liquid is known as mesophase and those materials which show a stable mesophase are classified as Liquid Crystals. The mesophase has properties of both liquid as well as solid state. Various properties such as electrical, thermal, optical and magnetic are inherited from liquid phase and a well defined lattice structure is inherited from crystalline phase. When the molecules are disc like shaped, they are termed as discotic liquid crystals and are of prime concern for the scope of this thesis work.

1.1 History

Liquid crystals are a century old and were first discovered by the Austrian chemist Friedrich Reinitzer. Reinitzer was trying to find the melting point of cholesterol based substances when he discovered that the molecules showed two melting points. Further German physicist Otto Lehmann investigated this phenomenon and classified these materials to be in an intermediate phase of matter and called these substances as Liquid Crystals. In the 1960s, Pierre-Gilles de Gennes[1], a

French theoretical physicist, who had been working with magnetism and superconductivity, developed his interest in the field of liquid crystals and soon found fascinating analogies between liquid crystals and superconductors as well as magnetic materials. He was awarded with the Nobel Prize in Physics 1991 for his work on Liquid Crystals and the modern development of liquid crystal science has since been highly influenced by his work.

Discotic Liquid Crystals are not that old as Liquid Crystals. The discovery of Discotic Liquid Crystal molecules is credited to Sivaramakrishna Chandrasekhar[2] *et.al.* who prepared these molecules and further characterized them in 1977. Finally the basic columnar structure of DLCs was verified by the brilliant x-ray work of Levelut[3] (1979, 1983). Discotic Liquid Crystal molecules have a flat core generally made up of fused benzene ring and alkyl chains attached to it. The flat core allows the stacking of these molecules in a columnar structure which enhance various property such as charge transport, effect of irradiation of polarized light and temperature gradient.

1.2 Classification of Liquid Crystals

On the basis of transition Liquid Crystal molecules can be classified as Thermotropic Liquid Crystals and Lyotropic Liquid Crystals. When the transition of phase from crystalline to liquid crystal and liquid is dependent upon the temperature, then these types of LCs are termed as **Thermotropic Liquid Crystals** wheras when the phase transition is dependent upon the concentration, they are called as **Lyotropic Liquid Crystals**. The thermotropic LCs have a rigid core with an alkyl chain attached to it whereas Lyotropic LCs have a soap like structure.

Liquid Crystals can also be classified on the basis of reversibility of phase. Enantiotropic Liquid Crystals show intermediate phase in both directions i.e, Solid-Mesophase-Liquid and Liquid-Mesophase-Solid whereas as Monotropic Liquid Crystals show mesophase in only one direction i.e, Liquid-Mesophase-Solid.

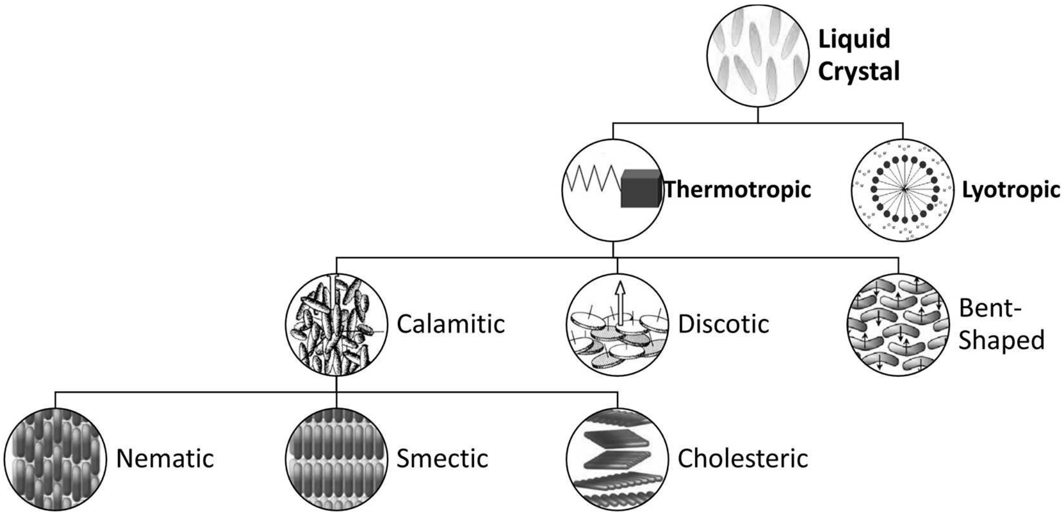

FIGURE 1.1: Classification of Liquid Crystal molecules.

Thermotropic Liquid Crystals also known as Non-amphiphilic can further be classified as in Smectic, Nematic and Cholesteric state. The **smectic** phase is a well ordered two dimensional state in which molecules stack together one upon other. The smectic phase is much closer to the solid like arrangement. Smectic phase has a layer like arrangement in which liquid crystals can move within the layers but movement of the layers is prohibited. The **nematic** phase is ordered in one dimension only and is more closer to the liquid phase and behaves differently when interacts with light and temperature. The materials in this phase are widely used in displays and temperature sensors. They are the least ordered liquid crystal molecules. The **cholesteric** phase is a special case of nematic liquid crystal and is named after the experiments of Reinitzer. These liquid crystals have a complex helical structure.

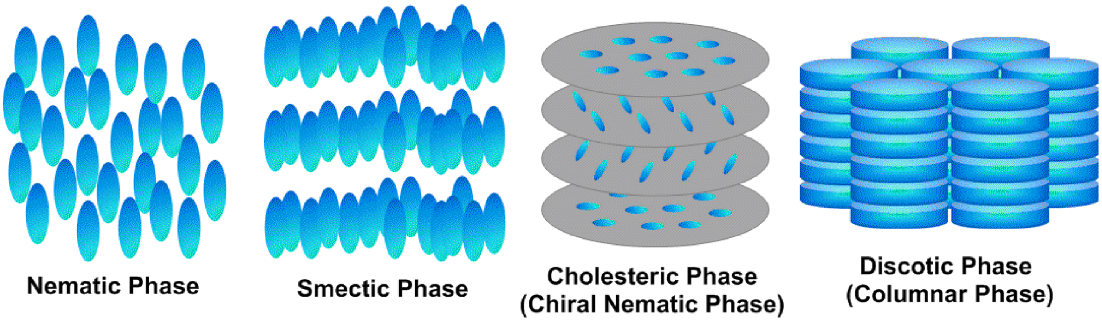

FIGURE 1.2: Classification of Liquid Crystal molecules on the basis of orientation [*ref:www.tcichemicals.com/eshop/en/cz/category˙index/12775/*].

1.3 Discotic Liquid Crystals

As mentioned above our prime research wok will revolve around the supramolecular assembly of discotic liquid crystal molecules. Various types of discotic liquid crystal molecules are shown in Figure 1.3. These materials generally consists of a flat and rigid aromatic core which is surrounded by a flexible alkyl chain attached with some functional group. These groups can be benzoate, ester, ether, imidazolium etc. The core can be benzene, triphenylene, pyrene, dibenzopyrene etc. The synthesis of these material is a straight forward job but purity of sample is of vital importance. As in assembling the core with the alkyl chain by aromatic substitution can result into incomplete substitution of some functional groups.

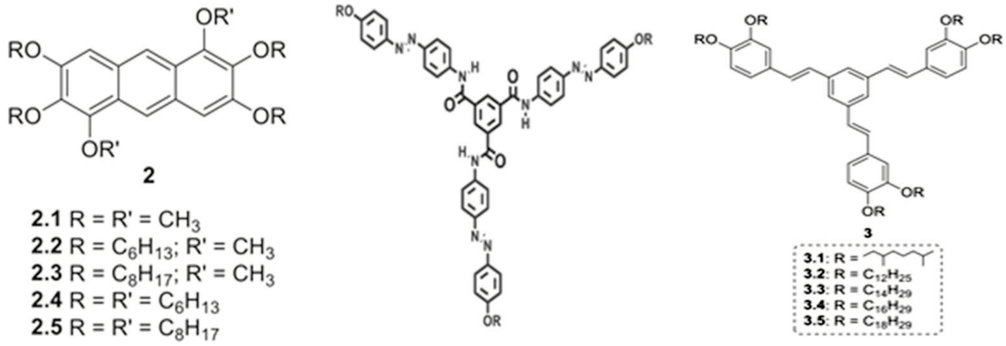

Figure 1.3: Various examples of Discotic Liquid Crystal molecules attached with different functional groups.

DLCs are of prime importance in organo-electronic devices and is a field of active research and development. Various fields in which scientific research have been moving with pace are electronic devices[4] such as photovoltaic devices, light emitting diodes, FETs and MOSFETs, sensors etc. One of the major application of DLCs is in memory based devices using Atomic Switches. An atomic switch is a device based on resistive switching phenomenon in which conduction takes place because of the atomic point contact formed by electrochemically active metal ions such as Silver, when a bias is applied across them.

DLC molecules have a property of self assembly[5] which makes the film highly ordered. This assembly governs the performance of organic electronic devices as the flow of charge is dependent upon film growth. Besides these, DLCs have a property of self healing and any defects can be self treated. One of the major property in DLCs is of highly interactive pi stacking[6]. The flat core which is made up of aromatic compounds forms pi stacking and as the separation between two pi stacked cores decreases, the charge transport property improves. The typical distance between two core of a DLC pair is of 0.35 nm. Different DLC molecules show different kind of pi stacking such as parallel, parallel-displaced or T-shaped pi stacking. These property of DLCs can also be tuned using various parameters such as effect of temperature, polarised light or surface concentration. Stacking of DLCs into a columnar structure can result into a 1-d conductor with a property of quantized conductance and can be described as molecular wires. The two dimensional arrangement can be utilized in devices like FETs and MoSFets as shown in Figure 1.4.

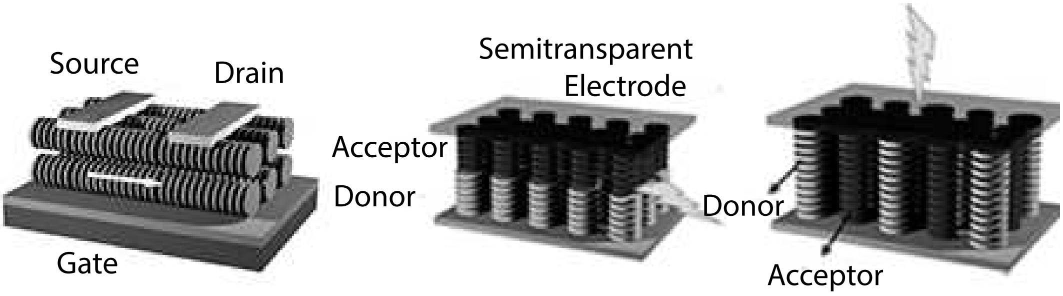

FIGURE 1.4: Application of Discotic Liquid Crystal molecules as a Field Effect Transistor, Light Emitting Diode and Photovoltaic Cell [*ref: Sergey Sergeyev et.al. Chem. Soc. Rev., 36:1902-1929, 2007.*]

1.4 Imidazolium Triphenyle Molecule

One such Discotic liquid crystal molecule is Imidazolium Triphenylene as shown in Figure 1.5. It is an amphiphilic molecule which means it consists of two groups i.e; a hydrophilic group and a hydrophobic group. The hydrophilic group is water loving and forms a good thin film on water surface whereas as the hydrophobic part stays away from water. These ImTp molecules are classified into neutral and ionic molecules as the arrangement of these molecules vary due to different ionic-ionic, ionic dipole and dipole-dipole interactions.

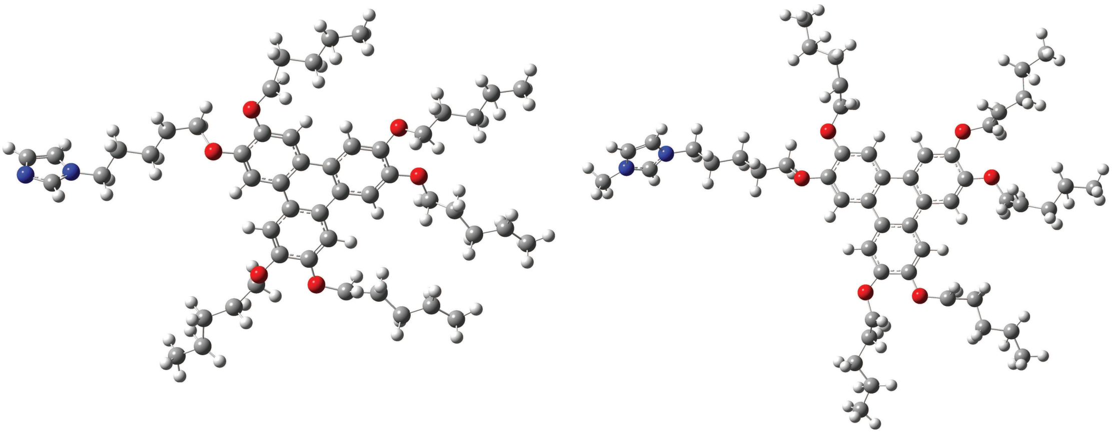

Figure 1.5: Energy minimized molecular Structure of neutral and ionic Imidazolium Triphenylene molecule.

Hydrogen bonding plays an important role in the arrangement of these molecules on surface of water. Because of these factors both neutral and ionic ImTp DLCs form a stable LB film over water surface. The molecules are also stable for a wide range of temperature ranging from 35° C to 85° C. The molecular weight of neutral ImTp molecule is of 811.14 g whereas the ionic counter part is of 827.19 g. The average dipole moment was of 9.679 and 39.195 Debye for neutral and ionic ImTp molecules respectively. The shape of these molecules are flat in nature and the surface area is of 5.73 nm^2 and 6.12 nm^2 respectively for neutral and ionic molecules. The ionic ImTP molecule has a positive charge on Nitrogen atom which is neutralised by adding a Bromine ion. The liquid crystalline property is also dependent upon the the counter ions, since the variation of Br^- to BF_4^- destroys the liquid crystalline property. The ionic ImTp molecule is one of the first known thermotropic liquid crystal and is of vital importance in paving the way for next generation organic electronic devices.

A theoretical study has been conducted on these molecules using Density Functional Theory and Molecular Dynamic Simulation to understand the supramolecular assembly of these molecules. A brief introduction to Density Functional Theory and Molecular Dynamics Simulations has been discussed in the next section.

1.5 Theoretical Techniques

1.5.1 Density Functional Theory

1.5.1.1 Introduction

Solving the Schrodinger equation can yield the exact energy and various other properties like bond length, atomization energy, heat of formation etc. of atoms and molecules. But in reality solving a many body problem using Schrodinger wave equation becomes impossible. Various approximations have been made to solve the Schrodinger wave equation for a many body problem. Such approximations include Ab initio method, Semi-empirical method and Density Functional Theory methods.

$$i\hbar\frac{\partial\Psi}{\partial t} = -\frac{\hbar^2}{2m}\frac{\partial^2\Psi}{\partial x^2} + V\Psi \tag{1.1}$$

As the name suggests Ab initio methods uses the position of nuclei and the number of electrons to solve the Schrodinger wave equation. This method do not considers any experimental value and can be used for small systems because of the huge computational cost. The major advantage of using Ab initio method is that if all approximations are small then the equation converges to the exact solution.

In Semi-empirical method huge amount of approximation is done such as core electron are not included, minimal basis sets are used and some times two electron integrals are also omitted. The advantage of Semi empirical method is that it is very fast in comparison to ab initio calculations and it also uses experimental data to compute the energy density values but a major disadvantage is that during approximations the results can be erratic and completely different from the actual ones.

Density Function Theory has become very popular in recent times because of its accuracy like ab initio method and computational speed like Semi empirical method. This method utilizes electron density function which is a function of some other functions to calculate the energy using Schrodingers wave equation. In this chapter how Density Functional Theory simplifies the Schrodinger equation without much affecting the output is dealt.

1.5.1.2 Born-Oppenheimer Principle

The very first approximation to solve the Schrodinger's equation came from Born-Oppenheimer approximation. The theory stated that the nuclear and electron part of Schrodingers equation can be solved separately as the mass of nucleus is 10^3 times higher than that of electron. So the degree of freedom for electronic Hamiltonian reduces to 3N where N is the number of electron. But a general solid consists of 10^23 electrons and solving such number of equation is not practically viable.

$$\psi_{total} = \psi_{nuclear} * \psi_{electronic}$$

1.5.1.3 Thomas and Fermi Theory

In late 1920 Thomas Fermi theory proposed a conceptual assumption of having electron density n(r) as the variable of prime importance rather than the number of electron wave functions. This method constrained the degree of freedom from many body to just three i.e; x, y and z.

$$E_K^0 = c_k n^{2/3} \sim 1/r_s^2, \qquad c_k = \frac{3}{10}(3\pi^2)^{2/3}. \tag{1.2}$$

$$K_0 = c_k \int d\mathbf{r}[\rho(\mathbf{r})]^{5/3}. \tag{1.3}$$

$$\mathcal{L} = \frac{1}{2}M\sum_{I=1}^{N_1}\dot{\mathbf{R}}_I^2 + \frac{1}{2}m\int d\mathbf{r}\dot{\rho}^2(\mathbf{r}) - E[\rho, \{\mathbf{R}_I\}] - \sum_J\sum_{I<J}\frac{Z^2}{|\mathbf{R}_I - \mathbf{R}_J|} + \mu\left\{\int d\mathbf{r}\rho(\mathbf{r}) - N_2\right\}. \tag{1.4}$$

1.5.1.4 Hohenberg and Kohn Theorem

Since the introduction of Schrodingers equation in 1926 it has become a challenge to solve it for many body problem. Just after two years of introduction to Schrodingers equation Dirac Stated that **”The underlying physical laws necessary for the mathematical theory of a large part of physics and the whole of chemistry are thus completely known, and the difficulty is only that the exact application of these laws leads to equations much too complicated to be soluble.”**

In 1964 Hohenburg and Kohn Theorem completely reformed the the way of approximating the Schrodingers equation and is reponsible for the modern day DFT calculations. The theorem relates any system consisting of electrons moving under the influence of an external potential $\mathrm{V}_{\mathrm{ext(r)}}$. The first Hohenberg -Kohn theorem states that the external potential energy and hence the total energy is a unique functional of electron density n(r).

The second Hohenberg-Kohn theorem states that the ground energy can be obtained variationally; the density that minimizes the total energy is the exact ground state density.

Even though Hohenberg-Kohn theorem is very powerful yet it can not be used to calculate energy of ground states and hence to calculate energy of the ground state Kohn-Sham Formulation was given one year later. This formulation is on which the modern day DFT works. The Kohn-Sham theorem maps all interacting systems with a potential on to the non-interacting system and the electrons move within an effective "Kohn-Sham" single particle potential.

$$K_L[\rho] = K_0(n) + \frac{1}{2}\sum_{\mathbf{k}}\sum_{\mathbf{k}'} \left.\frac{\delta^2 K}{\delta\rho_{\mathbf{k}}\delta\rho_{\mathbf{k}'}}\right|_n \delta\rho_{\mathbf{k}}\delta\rho_{\mathbf{k}'} = K_0(n) + \frac{1}{2}\sum_{\mathbf{k}} \chi_{id}^{-1}(\mathbf{k})\delta\rho_{\mathbf{k}}\delta\rho_{-\mathbf{k}} \tag{1.5}$$

1.5.2 Molecular Dynamic Simulations

Unlike Density Functional Theory, MD simulations do not use quantum mechanical phenomenons but classical Newtonian equations to predict the motion of atoms and thus the interactions taking place between them. These classical interactions can be summed up as

$$m \times a = F = -\frac{\partial U(r)}{\partial r} \tag{1.6}$$

In this process all forces acting on all the atoms are calculated and a numerical iterations take place yielding us the final system after certain time period.

1.5.2.1 Molecular Interactions

Various molecular interactions taking place can be broadly classified into three parts which are briefly described later. Suppose, these molecular interactions acting on N number of atoms, hence total degree of freedom becomes 6N (3 because of x, y, z coordinates and other three because of velocity components $\mathrm{v_x}$, $\mathrm{v_y}$, $\mathrm{v_z}$).

1.5.2.2 Non-bonded Interactions

The potential energy representing the non-bonded interactions can be split into many body terms as follow:

The term U(r) represents an external potential field and it also takes on pair potentials rather than three or many body interactions. The Lennard-Jones potential is most commonly used for of non-bonded interactions because of its simplicity and ease in calculations. The Lennard-Jones potential equation combined with Coulombic potential can be given as:

$$U_{ij,LJ} = 4\epsilon_{ij}\left(\left(\frac{\sigma_{ij}}{r_{ij}}\right)^{12} - \left(\frac{\sigma_{ij}}{r_{ij}}\right)^{6}\right) + \frac{q_i q_j}{r_{ij}} \tag{1.7}$$

Here, ϵ_{ij} is the potential well depth and σ is the distance at which potential becomes zero and r_{ij} is the intermolecular distance. The electrostatic forces if present can be given by Coulombic potential where $\mathrm{q_i}$, $\mathrm{q_j}$ are respective charges. These are long range forces and play an essential part in simulations.

1.5.2.3 Bonded Interactions

Various kinds of bonded interactions such as dihedral potential, bond potential, angle potential are obtained from the vibrational analysis. The bonded interactions are considered between three vectors i.e; r_{ij}, r_{jk} and r_{jk} for three atoms. A typical force fields file is generated using various tools such as topolgen[7], lig par gen etc. and hence, various strength parameters like k and other constants are calculated. The iteration of these force over the time period on all atoms gives us the precise motion of molecules.

$$\begin{aligned} U_{intramolecular} = {} & \frac{1}{2}\sum_{bonds} k^{r}_{ij}(r_{ij} - r_{eq})^2 + \frac{1}{2}\sum_{bendangles} k^{\theta}_{ijk}(\theta_{ijk} - \theta_{eq})^2 \\ & + \frac{1}{2}\sum_{torsionandles}\sum_{m} k^{\phi,m}_{ijkl}(1 + \cos m\phi_{ijkl} - \gamma m) \end{aligned} \tag{1.8}$$

1.6 Experimental Techniques

1.6.1 Langmuir Blodgett Technique of Film Deposition

Langmuir[8] Blodgett[9] technique is a process of depositing a monolayer (one molecule thick) or a set of monolayers of film, generally composed of organic materials on a solid substrate. By using this method the thickness of film can be controlled precisely on the solid substrate.

The process by which LB film deposition takes place is briefly dealt in this section. The important parts on LB system consists of a trough top, barriers, frame, a surface pressure sensor, a dipping mechanism and an interface unit. The LB trough includes a dipping well and a pair of barriers. Barriers are motorised and as they move closer to each other the concentration of surfactants increases. A dipping mechanism is placed just above the trough well for substrate dipping. The sensors and balance are used to measure the surface pressure and are connected to the computer through interface unit. The thickness of film depends upon the air water interface and hence the surface pressure. Thus, the thickness of film deposition on substrate can be controlled by varying barrier position and number of dips. Langmuir Blodgett technique of thin film deposition is one of the best method for monolayer or set of monolayer deposition as we can control the number of molecules deposited on the substrate accurately.

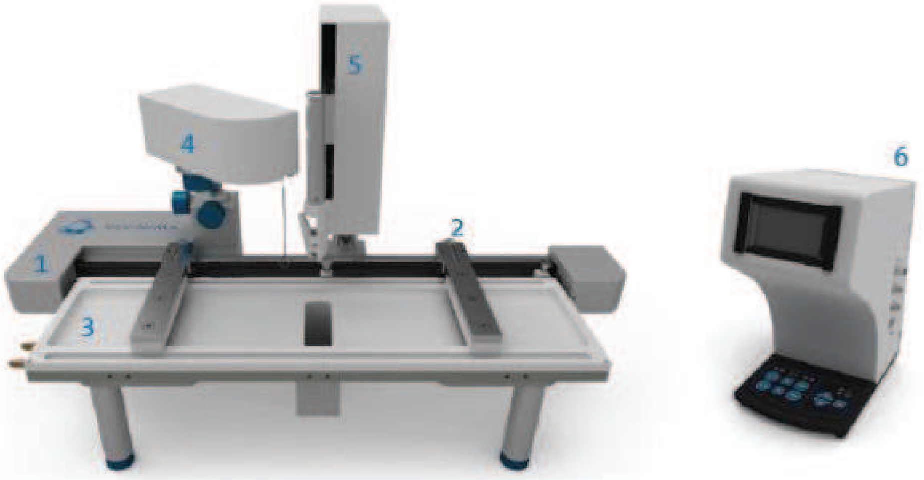

FIGURE 1.6: Vaious components of Langmuir Blodgett System for thin film deposition [*https://www.biolinscientific.com/ksvnima*]

Various parameters such as Surface Manometry, Transfer Ratio, Brewster Angle Microscopy, Reflection Microscopy etc. are used for measuring and characterising the LB film. In this research thesis work surface Manometry and Transfer ratio measurements were taken and are briefly discussed here. Surface Manometry is a process in which we plot surface pressure (π) as a function of area per number of molecules ($\mathrm{A_m}$). Here surface pressure (π) is the difference between the surface tension of water without monolayer and with monolayer. As the barriers move the surface area per number of molecule is varied and hence the surface pressure varies as its function. This plot is also commonly known as π-$\mathrm{A_m}$ isotherm as the temperature is kept constant during this plot. The Transfer Ratio can be defined as the ratio between the area of substrate covered by the molecule to the total surface area of the substrate. This technique gives us the information about how much sample is deposited on the substrate and its property to stick on the substrate.

1.6.2 Scanning Probe Microscopy

Scanning Probe Microscopy is a remarkable method which gives us the ability to view the surface at atomic and molecular level. Atomic Force Microscopy is a SPM method in which the AFM tip experiences van der Waals force when brought very close to the sample. When the tip is brought at an intermolecular distance with respect to the sample it may experience other force due to magnetic field, electrostatic charge etc. but the magnitude of van der Waals force is quiet high in comparison to these forces.

Atomic Force Microscopy was discovered by Binning et al. in 1986, the co-discoverer of Scanning Tunnelling Microscope[10] to overcome the limitation of STM which was only confined for conductive surfaces. AFM is based on measuring the deflection of cantilever when brought closer to the sample at intermolecular distance. The cantilever experiences a force because of the van der Waal interaction and hence the cantilever gets deflected. The Deflection of cantilever is measured with the help of a laser beam. The laser beam is incident on the cantilever and is reflected back on the four quadrant photovoltaic detector. The voltage measured by the photo diode detector is converted into deflection of cantilever using the following equations:

$$y_{def} = (A_1 + A_2) - (B_1 + B_2) \tag{1.9}$$

$$x_{def}(torsion) = (A_1 + B_1) - (A_2 - B_2) \tag{1.10}$$

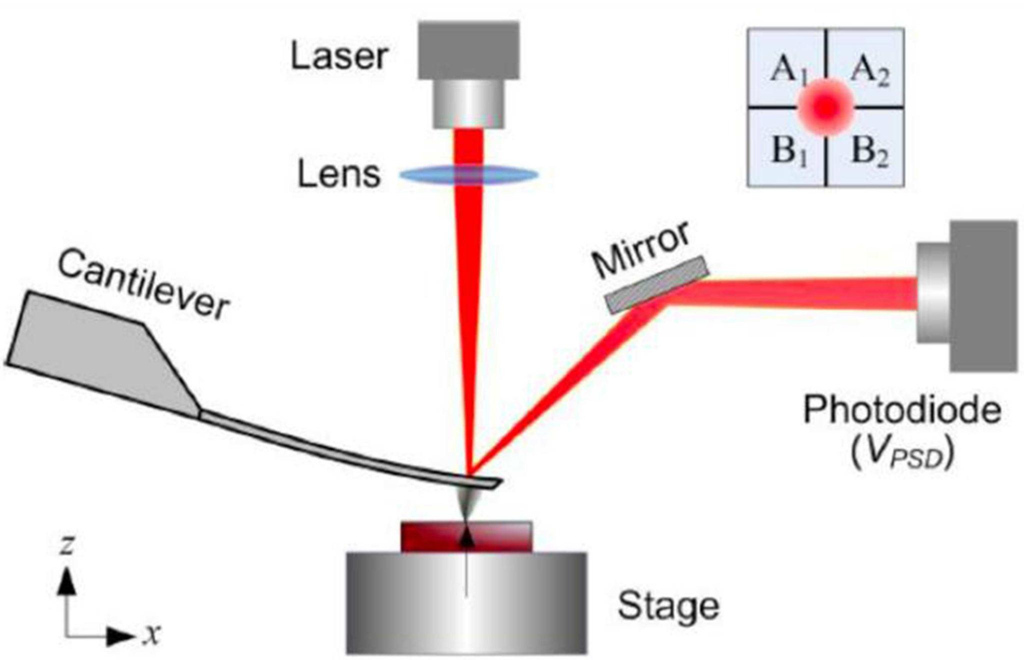

Figure 1.7: Optical lever deflection method for the detection of the cantilever bending in Atomic Force Microscopy[*ref: Georg Fantner: Advanced Bioengineering Methods Laboratory, Atomic Force Microscopy*]

Here strictly speaking, the deflection of cantilever along the z axis is not taken into consideration but the angle of the neutral axis of the deflected cantilever. The angle of deflection is directly proportional to the cantilever deflection in z axis and finally proportion to the Force(F).

$$F = k_x \Delta z = (3EI/L^3)\Delta z \tag{1.11}$$

Where k_x is the stiffness of cantilever which is dependent upon E (Elastic Module), I (Moment of Inertia) and L (length of cantilever).

Also the displacement of tip is a function of the z displacement of the neutral axis $w(x)$.

From the deflection angle θ force can be calculated as:

$$\theta = dw(L)/dx = FL^2/2EI$$

Therefore,

$$F = (2EI/L^2)\theta \tag{1.12}$$

AFM has a lot of application in field on nano science and nanotechnology as it can not only be used for taking images of sample but for measuring I-V characteristics, force vs Distance plot and also as nanoscopic tool for lithography, cutting and extracting soft molecules at sub micron level. Besides this, AFM finds application in study of biological samples at a nanoscale level.

Chapter 2

Experimental Insight

2.1 Objective

The prime objective of our experimental work was to study the self-assembly of neutral and ionic ImTp molecules at air-water and air-solid interfaces. In order to study the self-assembly at air-water interface, surface manometry technique was used and to study the self-assembly at air-solid interface, atomic force microscopy was used.

2.2 Experimental Process

The neutral and ionic ImTp molecules were synthesized by Pal *et.al.* at the Raman Research Institute, Bangalore. The materials were purified by repeated recrystallizations with diethyl ether and characterized by 1H NMR, 13C NMR, IR, UV spectroscopy and elemental analysis which indicated high purity (99%) of the materials. The thermotropic liquid crystalline properties of the materials were investigated by polarizing optical microscopy and differential scanning calorimetry. The neutral ImTp material does not show any liquid crystalline phase. On heating, the material directly goes from crystalline phase to isotropic liquid phase at 50°C. On the other hand, the ionic ImTp material in the bulk exhibits liquid crystalline phase and has the following phase sequence: solid-columnar at 67°, columnar-isotropic at 101°. On cooling, the columnar mesophase appeared at 98° with the mesophase solidifying at 38°. The details of synthesis and characterisation of these materials are reported elsewhere[11].

For studying supramolecular self-assembly of these molecules, first, Langmuir monolayers were formed and then, the monolayers were deposited onto silicon substrates using Langmuir-Blodgett (LB) technique. The subphase used was ultra-pure deionized water obtained from Millipore Milli-Q system. The materials were dissolved into HPLC-grade chloroform and their stock solutions of 0.236 mM concentration were prepared. The stock solutions were spread slowly on the water surface drop by drop using Hamilton syringe. The system was left for 30 minutes for the stock solution to spread all around the water surface and also the chloroform evaporates during this time. The isotherm data were obtained by the symmetric compression of barriers. The compression rate was fixed to 0.103 nm^2/molecule/min. For LB film deposition, the dipping speed was kept fixed at 2 mm/min. The depositions were carried out on hydrophobic silicon surface. To make the silicon surface hydrophobic in nature, it was first made hydrophilic by treating it with hot piranha solution for about 3 minutes. Piranha solution is a mixture of conc. H_2SO_4 and H_2O_2 in a ratio of 3:1. After the treatment with piranha solution, the substrate was rinsed with ultra pure deionised water and was dried at room temperature to obtain hydrophilic surface. Finally, the silicon substrate, after hydrophilic treatment, was dipped into HMDS for 12 hours and then cleaned with HPLC grade chloroform to obtain hydrophobic surface.

The atomic force microscope (AFM) was used to obtain the topography images of these samples deposited over hydrophobic silicon substrates. The tips used to get the images had a spring constant of 21 N/m and a resonance frequency of 250 kHz. The tips used were made up of silicon and the images were obtained in non-contact mode. The images were processed using WSxM and only image flattening was done to remove some noise induced due to electrical and stray magnetic factors.

All experiments were performed at room temperature and in ambient condition for both neutral and ionic ImTp molecules.

2.3 Results and Discussion

2.3.1 Surface Manometry

The isotherm plots for the monolayers of neutral and ionic ImTp molecules at air-water[12] interface are shown in (Figure 2.1) and (Figure 2.2), respectively. The surface pressure starts to increase as the barriers move close to each other since the number of molecule per unit area increases. As the concentration of molecules increases, the monolayer undergoes phase changes and finally collapses at a critical concentration of molecules. In case of neutral ImTp molecules, the first rise in surface pressure was observed at a surface area per molecule of about 2.5 nm^2/molecule, whereas in case of ionic counterpart, the rise was observed at about 3.5 nm^2/molecule. Interestingly, the ionic molecules exhibited two phases, i.e., the expanded phase and condensed phase, whereas in the case of neutral molecules, only one stable phase was observed. This phenomenon can also be verified from the compressional elastic modulus plot which is discussed later.

For both the molecules, the increase in surface pressure was a linear phenomenon after the initial rise until the collapse of film took place. However, the slope of surface pressure w.r.t the surface area was higher and the limiting area per molecule was lower in case of neutral ImTp molecules. The limiting area was 1 nm^2/molecule for the condensed phase of neutral molecules, whereas for the ionic molecules, it was 1.4 and 3.4 nm^2/molecule for the condensed and expanded phase, respectively. Comparing their collapse pressures, it was observed that the collapse took place at a higher value of surface pressure for the ionic molecules than that of the neutral molecule. For ionic molecules, it was of 43 mN/m whereas for neutral molecules, it was of just 36 mN/m.

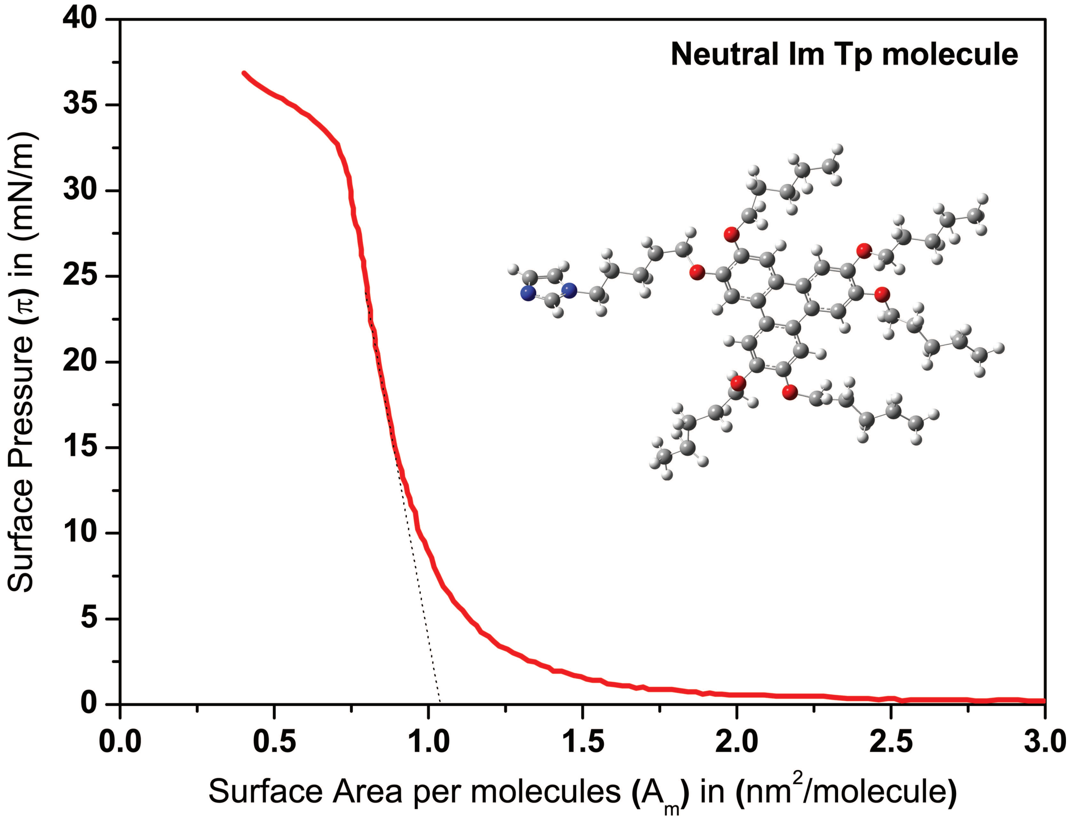

FIGURE 2.1: Isotherm plot for neutral ImTp molecule

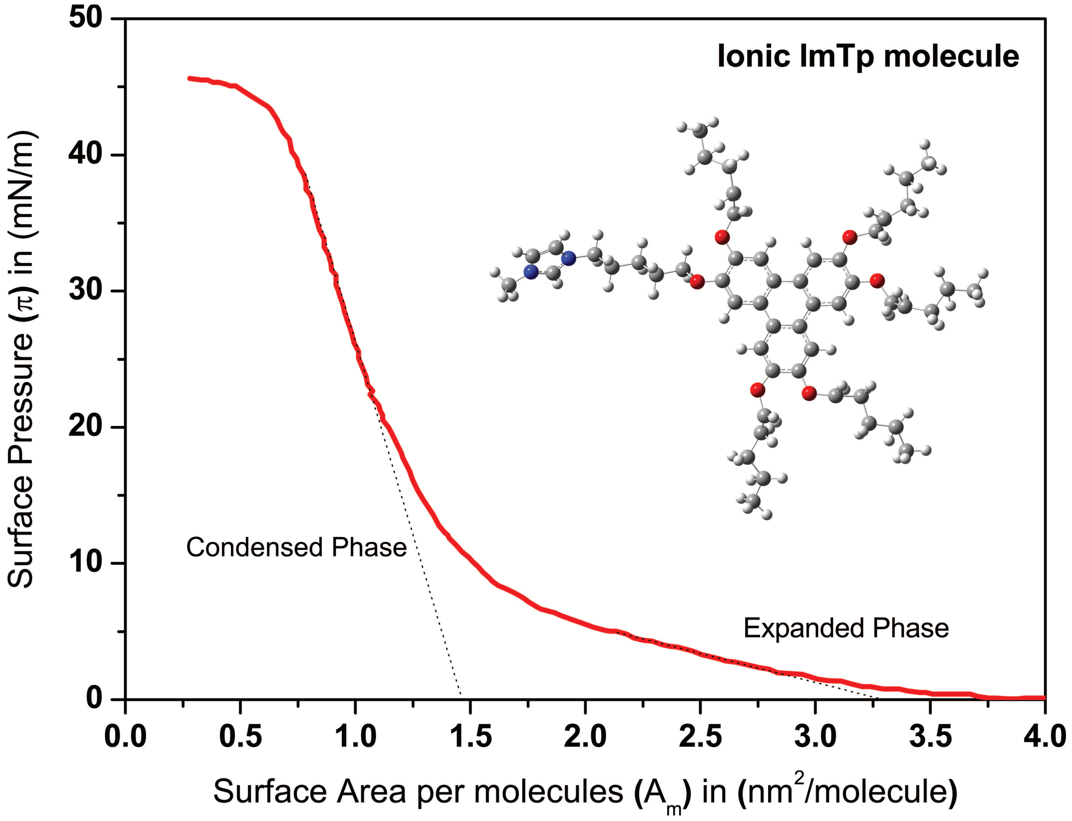

FIGURE 2.2: Isotherm plot for ionic ImTp molecule

The compressional elastic modulus for neutral and ionic ImTp molecules were calculated using the equation given by

$$|E|= A_m[\frac{d\pi}{dA_m}] \tag{2.1}$$

Here E is the compressional elasticity, π is the surface pressure and A_m is the area per molecule. The variation of compressional elastic modulus |E| for neutral and ionic ImTp molecules as a function of area per molecules A_m is shown in Figure 2.3 and Figure 2.4 respectively. The maximum value of compression elasticity for neutral molecules was of 75.7 mN/m at the surface area per molecule of 0.65 nm^2. This suggest that there are two stable phases for these molecules each at a surface area per molecule of 0.98 nm^2 and 1.25 nm^2 with the compressional elastic modulus |E| of 52.56 mN/m and 44.48 mN/m respectively.

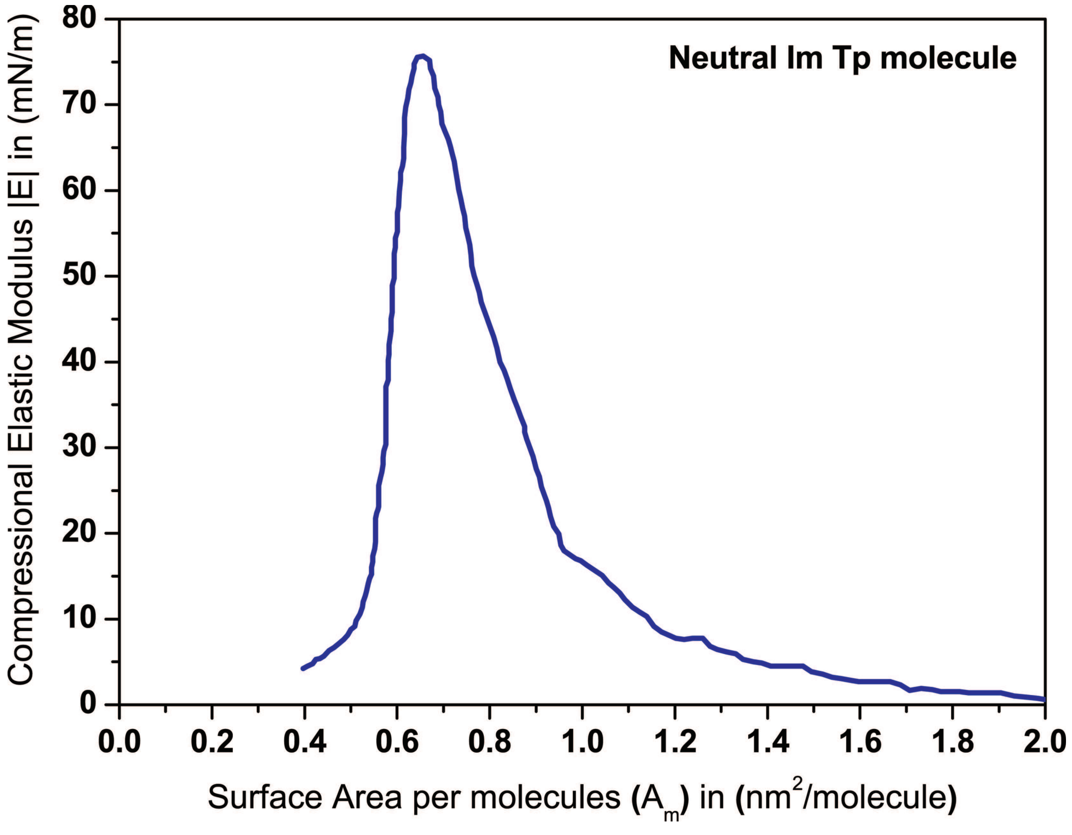

FIGURE 2.3: Compressional elastic modulus plot for neutral ImTp molecule

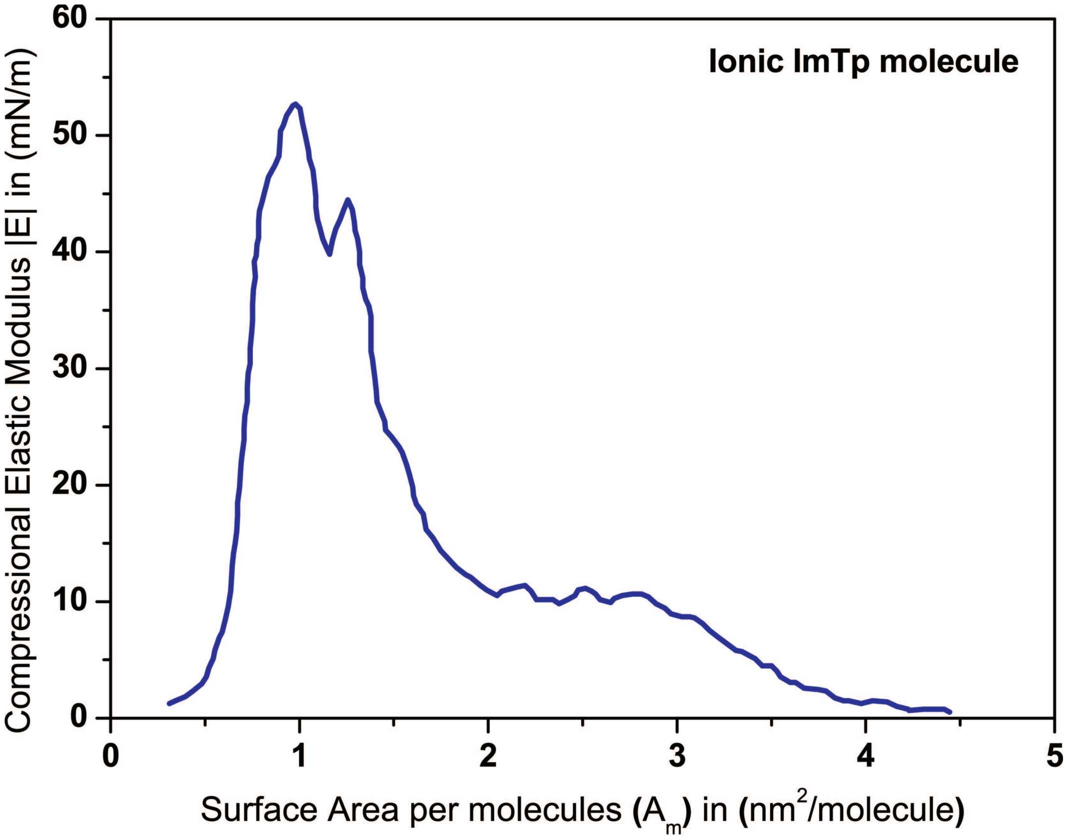

FIGURE 2.4: Compressional elastic modulus plot for ionic ImTp molecule

2.3.2 Atomic Force Microscopy

Neutral and ionic ImTp molecules, transferred on hydrophobic silicon substrates using the LB technique of film deposition, were scanned using AFM. The hydrophobic silicon substrates (AFM images shown in Figure 2.5) were deposited with two layers of neutral and ionic ImTp molecules. The height of the film was around 4 nm w.r.t substrate when deposited with neutral ImTp molecules at a surface pressure (π) of 27 mN/m corresponding to the condensed phase. Whereas, the height profile for ionic molecules showed the height around 5 nm w.r.t the substrate for the film deposited in the condensed phase. It is interesting to note that, despite similar chemical structures of both the types of molecules, the ionic molecules form thicker film by about 1 nm as compared to the neutral ones. The AFM images along with the line profile for both neutral and ionic ImTp molecules are shown in Figure 2.6 and Figure 2.7. In addition, a close view on the morphology of the film top surface revealed that the surface of ionic film was much more rough compared to that of the neutral film. The 2D and 3D images of the surface morphology are shown in Figures. These observations suggest that there is a difference in packing of molecules in ionic and in neutral ImTp molecular films.

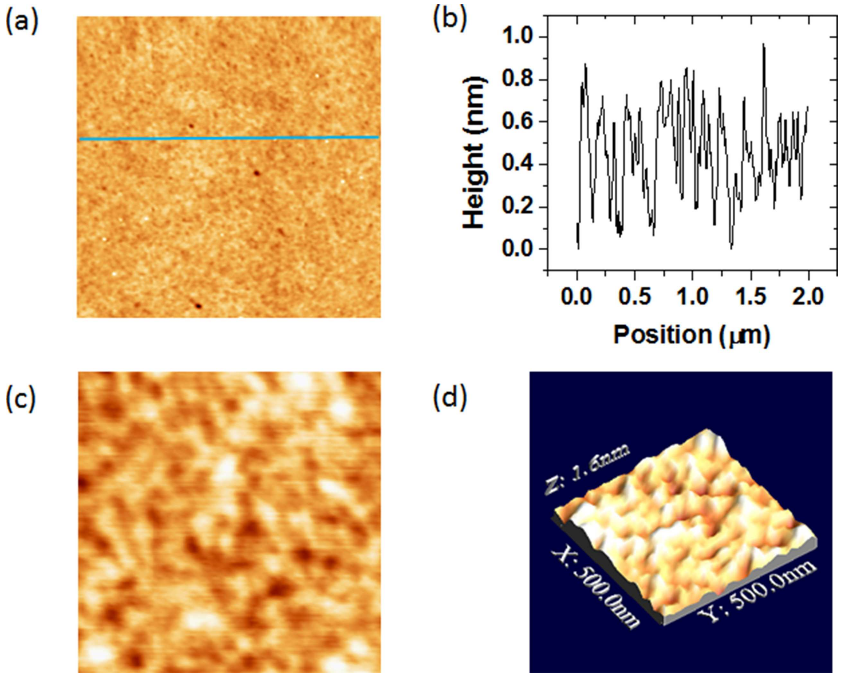

FIGURE 2.5: (a) AFM topography image of bare silicon surface ($2 \times 2\,\mu m^2$) with hydrophobic treatment. The rms roughness of the surface is 0.25 nm. (b) The height profile corresponding to the line drawn on the image showing roughness of the surface. (c) 2D image ($0.5 \times 0.5\,\mu m^2$) and, (d) its corresponding 3D image of a smaller scan area for better clarity.

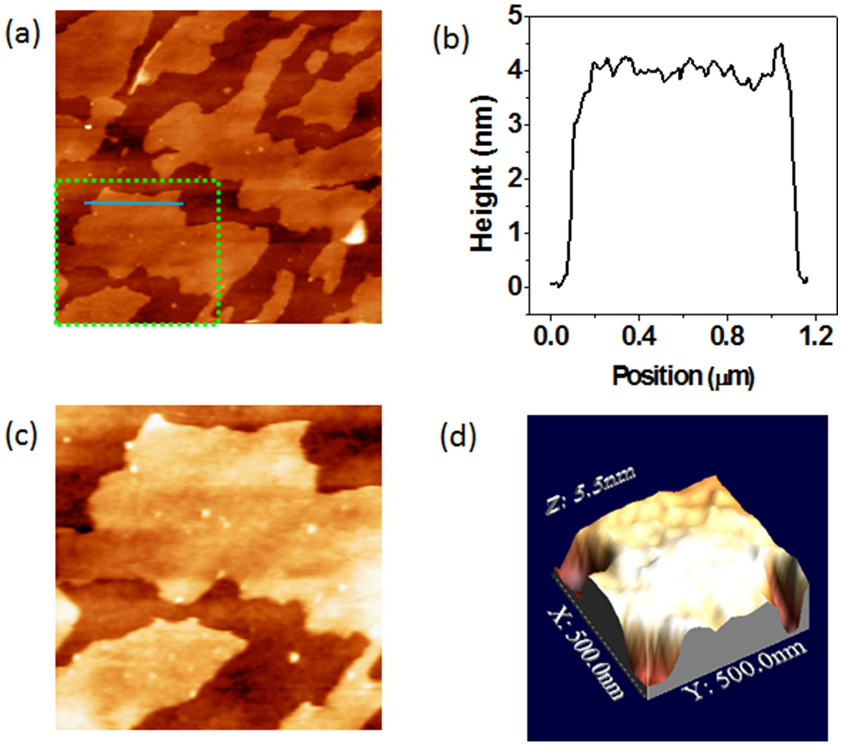

Figure 2.6: (a) AFM topography image of LB film with 2 layers of neutral ImTp molecules($3 \times 3\,\mu m^2$). (b) The height profile corresponding to the line drawn on the film showing thickness of about 4 nm. (c) 2D image ($1.5 \times 1.5\,\mu m^2$) and, (d) 3D image of a smaller scan area showing smooth top surface.

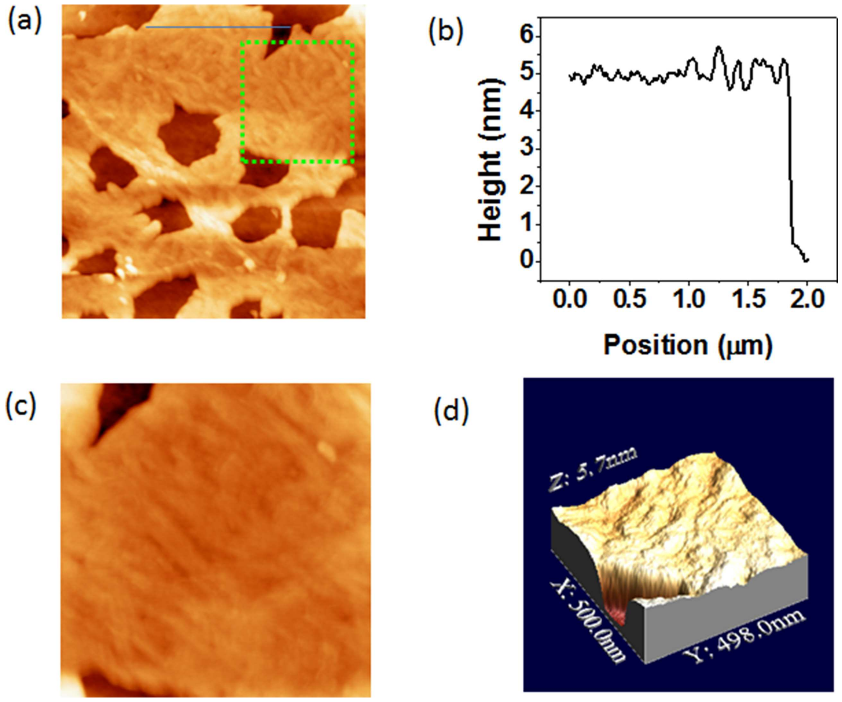

Figure 2.7: (a) AFM topography image of LB film with 2 layers of ionic ImTp molecules($4 \times 4\,\mu m^2$). (b) The height profile corresponding to the line drawn on the film showing thickness of about 5 nm. (c) 2D image ($1.5 \times 1.5\,\mu m^2$) and, (d) 3D image of a smaller scan area showing rough and undulated top surface.

2.3.3 Transfer Ratio

Transfer Ratio (τ) is defined as the surface area of a Langmuir monoloyer deposited on the substrate to the total area of the substrate. The Transfer ratio as function of number of layers obtained during the deposition on a hydrophobic silicon substrate for neutral and ionic ImTp molecules are shown in Figure 2.8. Higher value of τ signifies a better deposition of film. The maximum value of τ can be of unity and it denotes the best deposition. The film transfer was done at a dipping speed of 2 mm/min and the target surface pressure was held constant in the condensed phase for both neutral and ionic ImTp molecules. For the hydrophobic substrate, the hydrophobic part of the amphiphile gets attached to the substrate.

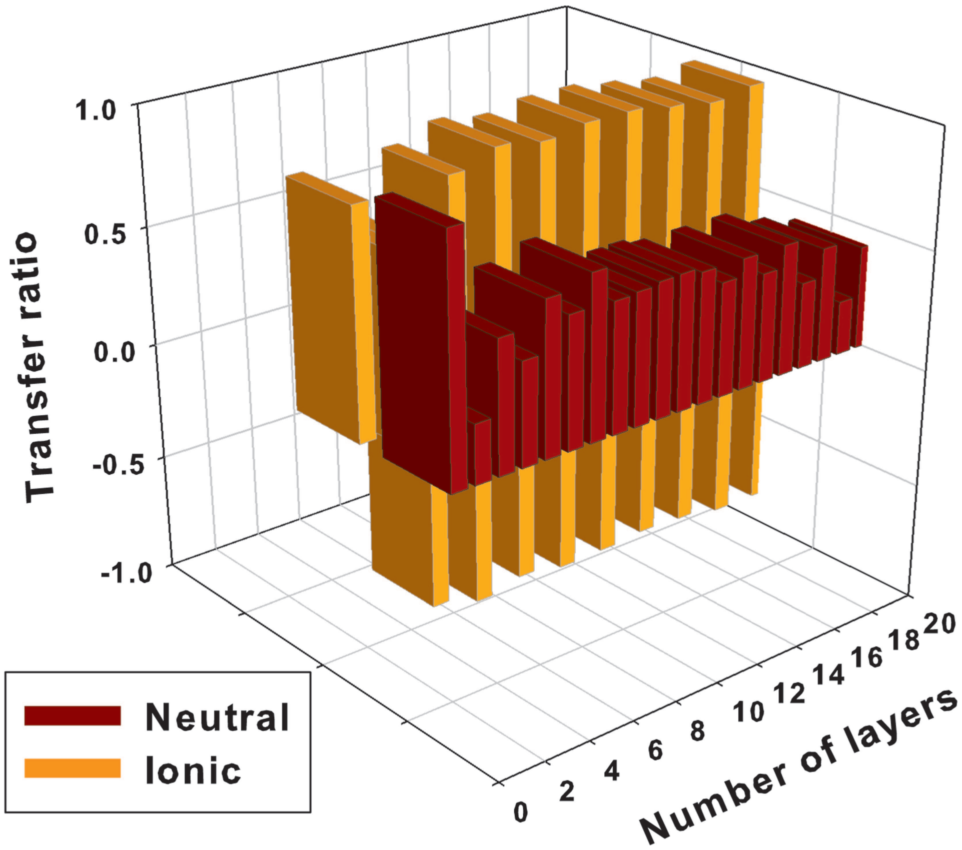

Figure 2.8: Tranfer ratio for neutral and ionic ImTp molecules on hydrophobic silicon surface as a function of number of layers

For the first down stroke, the transfer ratio was found to be of unity but as the number of layers increases the value of τ tends to decrease. However in case of neutral ImTp molecules the value of τ was significantly higher than the ionic ImTp molecules. Neutral ImTp molecules showed good transfer ratio upto 20 layers of depositions. Whereas in case of ionic ImTp molecule the deposition after the 2^{nd} layers was difficult as the negative value of τ indicates that the molecules were transferred from substrate back to the LB trough.

2.3.4 Conclusion

Surface manometry results show that neutral ImTp molecules had a lower limiting area and they collapsed at a lower surface pressure when compared with the ionic counterpart. AFM observations suggests that the height of film in neutral ImTp molecules was lower than that of ionic ImTp molecules. The average difference between the film thickness was of 1 nm. Also, the neutral ImTp molecules had a smoother and sharper surface w.r.t the ionic molecules. Further from the transfer ratio, it was observed that the deposition of neutral ImTp molecules on hydrophobic silicon substrate was relatively much easier than ionic ImTp molecules. For the first deposition of film on hydrophobic silicon substrate, the transfer ratio was found to be unity for both neutral and ionic molecules. But afterwards for ionic ImTp molecules, the transfer of film on silicon substrate was poor.

These experimental observations suggests that due to the presence of ionic polar head group in ionic ImTp molecules, there is a difference in molecular packing of these molecules. This difference in molecular packing further affects the self assembly and stacking of these molecules at air-water and air-solid interface.

LB film deposition is a complicated process both physically and chemically by nature and has been discussed with the help of theoretical modelling in the next chapter.

Chapter 3

Theoretical Modelling

3.1 Objective

The objective of DFT calculations for neutral and ionic ImTp molecule was to study the individual optimized structures and the various interactions taking place between two parallely placed ImTp molecules in gas phase. Further, MD simulations were performed to study the supramolecular assembly of these molecules on the surface of water at different surface to molecule concentrations.

3.2 Simulation Process

The initial structure for neutral Imidazolium Triphenylene molecule was built using Avogadro-1.2.0n software [13] and optimized using the inbuilt mmff4s forcefield. To reduce the computational cost the carbon chains were reduced to methyl groups only. The molecule was replicated into two and placed at an inter-planar distance of 3 Å using gaussview [14]. The final gaussian input file was submitted to gaussian[15] 16 for energy minimization. DFT calculation method using B3LYP [16–19] optimization was used with 6-311G++ basis set. The energy minimized structures obtained after DFT optimization were further analysed. The separation between two energy minimized molecules was tuned using gaussview and different

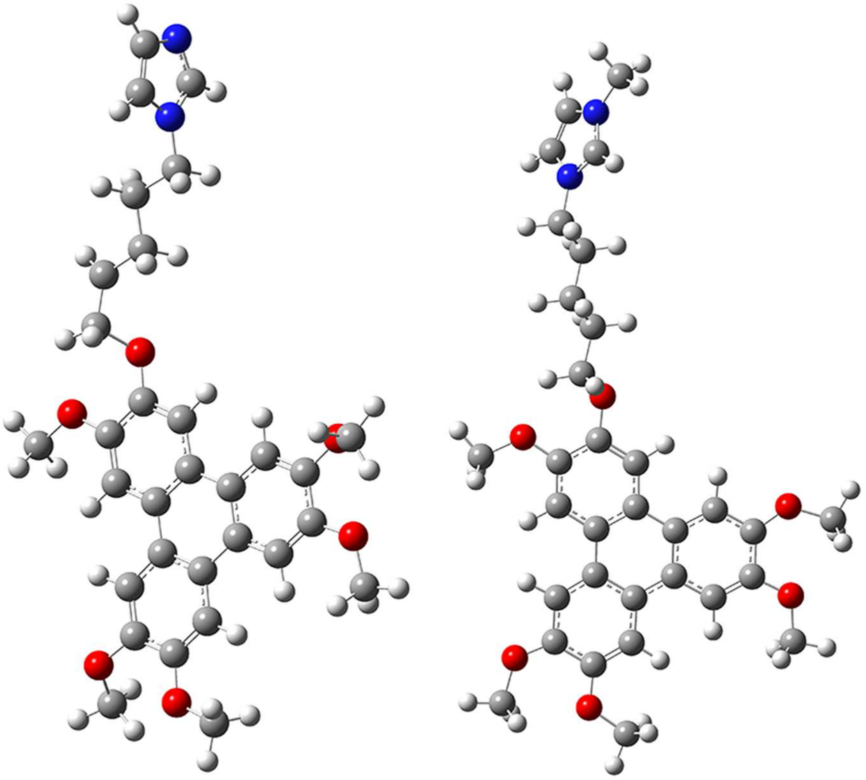

Figure 3.1: Reduced and optimized structure of neutral (left) and ionic (right) ImTp molecule

input files were created. For each input file, Single Point Energy (SPE) calculations were done and interaction energy in Kcal/mol was plotted as function of separation between the two molecules. The same process was repeated for ionic counter part and the results obtained were analysed.

MD simulations using GROMACS [20] were carried out to obtain the supramolecular assembly of neutral and ionic discotic molecules on the surface of water. The optimized structure of neutral and ionic molecules obtained from DFT calculations served as input file for this system. Along with these molecules standard SPC/E forcefield model of water was used. In case of ionic ImTp molecules to neutralize the system bromine ions (Br^-) were added. Molecular dynamic simulation were carried out on four systems with different surface areas based on the isotherm data obtained from the experiment discussed in Chapter 2. Packmol was used to build the initial configuration consisting of water (SPC/E model) and ImTp molecules as shown in Figure 3.2. A periodic box was created along x,y and z axis with a fixed length on 100 Å along Z-axis whereas the surface area of box along x and y dimensions were varied to change the surface concentration of Im Tp molecules. The depth of water was fixed to 15 Å (on average 7 layers of water molecules). All the systems consisted of 10 ImTp molecules placed on the surface of water such that the Imidazolium group (head group) is kept on water surface. The dimensional configuration for each system is shown in (Table 3.1).

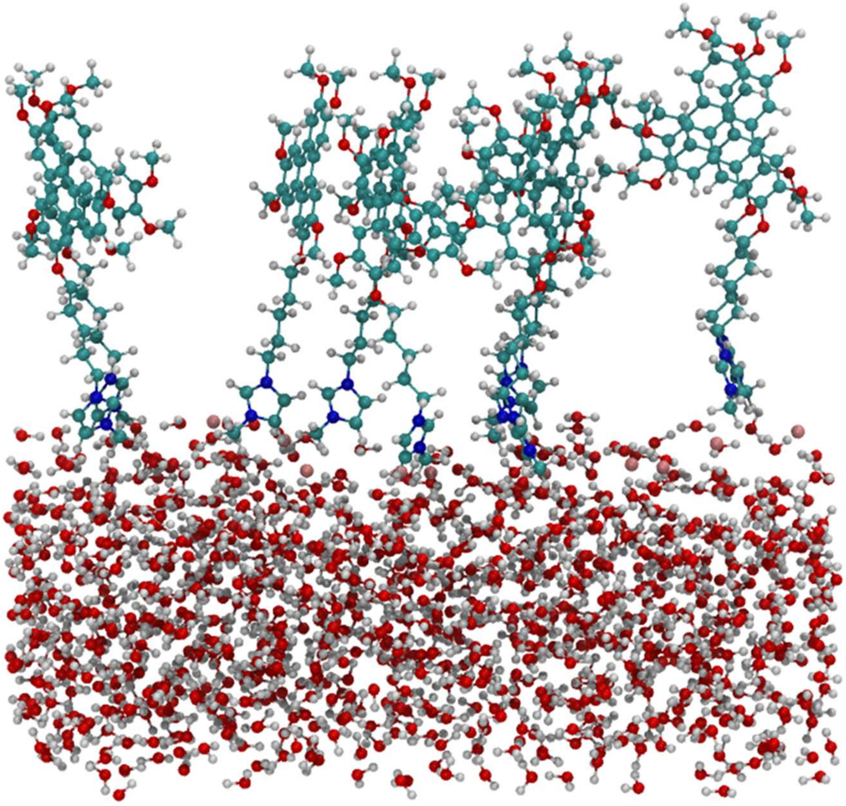

FIGURE 3.2: Initial structure of a 0.75 nm^2/mol surface area system for ionic IMTP molecules generated from Packmol

TABLE 3.1: Initial configuration for systems at different concentration of molecules used for neutral and ionic system generated from Packmol for MD Simulations

Surface Conc(nm^2/mol)	Area ($Å^2$)	No. water mol
0.5	22.36 X 22.36	247
0.75	27.37 X 27.37	370
1	31.62 X 31.62	493
1.5	38.73 X 38.73	740
2	45 X 45	1000
3	54.77 X 54.77	1480

Table 3.2: Lennard Jones parameters for water and Bromine ion used in Molecular Dynamic Simulations

atom/ion	epsilon (KJ/mol)	sigma (nm)
H	0.00000	0.00000
O	0.31660	0.65000
Br	0.42800	2.97064

OPLS-aa Force field generated from Lig Par Gen Server [21–23] were obtained for the energy minimized state of these molecules. The standard force field for water [24] and Bromine [25] ion are shown in (Table 3.2). The system was kept at a temperature of 298 K with all bonds held constraint using LINCS [26] algorithm. All the four systems were MD simulated for over 35000 time steps under identical conditions. The long-range electrostatic interactions were depicted using the particle mesh Ewald [27, 28] (PME) method of fourth order. The cut-off radius for the Lennard-Jones interactions and for the real part of PME calculations were set to 0.9 nm. All system were first nvt equilibrated for 2 ns and MD simulated for 7 ns.

The data obtained from the MD simulations were stored at a time step of 2 ps and respective trajectory files were obtained. All analysis such as Z Orientation, Z Density, Average number of hydrogen bonds were done using Gromacs utility [29] tools. All MD simulation results were visualised using VMD [30] and saved using Tachyon[31]. Gas phase Single Point Energy of these molecules with a hydrogen bonded single water molecule was also calculated using DFT calculations.

3.3 Results and Discussion

3.3.1 Gas Phase DFT Calculations

The optimized structure obtained from DFT calculations show that pi stacking was a dominant phenomenon among these molecules. The stacking of these molecules can be explained due to the presence triphenylene group present at the core, which is a well established fact for aromatic molecules. The inter planar distance between the two pi stacked cores defines the charge transport property and thus, a closely stacked discotic liquid crystal molecule offers better flow of charge. Hence, the property of high charge carrier mobility makes them a suitable component for organic electronic devices.

The DFT calculation show that the optimized interplanar distance between the neutral molecules was of 7.72 Å whereas for the ionic counter part it was of 9.77 Å. This can be justified because of the presence of electrostatic repulsion found in ionic molecules. The electrostatic repulsion because of the presence of ionic polar head group in ionic ImTp molecules was so strong that they showed T-shaped pi stacking. The centroid angle for T-shaped stacking was of. But due to the absence of any charge in neutral ImTp molecules, a parallelly displaced pi stacking was observed. The DFT optimized structures is shown in Figure 3.3. These observation can also be justified from the AFM images obtained in the experimental part of this research work. The AFM images for neutral molecules were sharp and smooth whereas the ionic molecules showed deposition in patches and were rough. Also, scratching of these molecules to obtain the film thickness was quite difficult as these films were rigid and highly stable.

Also, the interaction energy in case of T-shaped pi stacking was found out to be more stable than in case of parallel displaced neutral molecules. The difference of interaction energy between neutral and ionic molecules was calculated to be 4.49 Kcal/mol. The plot showing interaction energy as function of separation between two molecules is shown in (Figure 3.4). Broadly speaking, the stability of T-shaped pi stacking is much better than that of parallel displaced or parallel stacking because of the absence of electron-electron repulsion. In case of benzene dimer the interaction energy for parallel displaced stacking is higher than that of T-shaped pi stacking[32]. Therefore, stacking in case of neutral molecules are more compact but the stability in ionic counter part is much higher.

There were total 35001 frames obtained for a time span of 7 ns from the Molecular dynamic simulations and were analysed using GROMACS utilities. Various

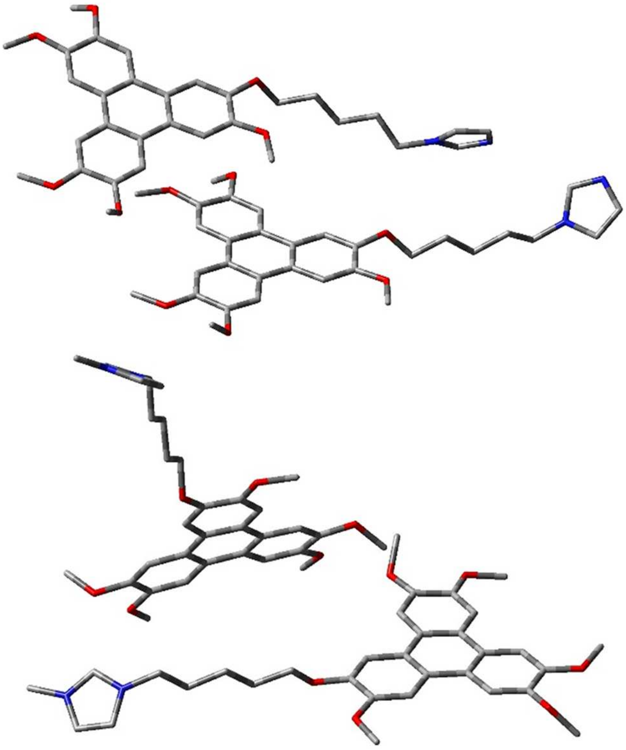

FIGURE 3.3: Optimized interplanar structure of neutral and ionic IMTP molecules in gas phase

analysis such as Z-Orientation, Z -Density and Hydrogen Bonding were calculated and are reported here.

3.3.2 Z-Orientation

The average angle of orientation of neutral and ionic molecules along with Z-axis was calculated to determine the orientation of these molecules on water surface. The vector for which these calculations were performed is shown in (Figure 3.5). Various atoms are also labelled along with the vector for which the system was analysed. The vector considered for Z-Orientation was taken between **C1** and **C2** atoms. The angle between vector C1 C2 and Z-axis is denoted by θ and was calculated for each ImTp molecule during the MD run. The bin value was calculated for different values of θ as a percentage of molecule. Therefore, the percent of molecules aligned as a function of θ was plotted. The Z-Orientation plot gives us the information about the ordering of ImTp molecules at different

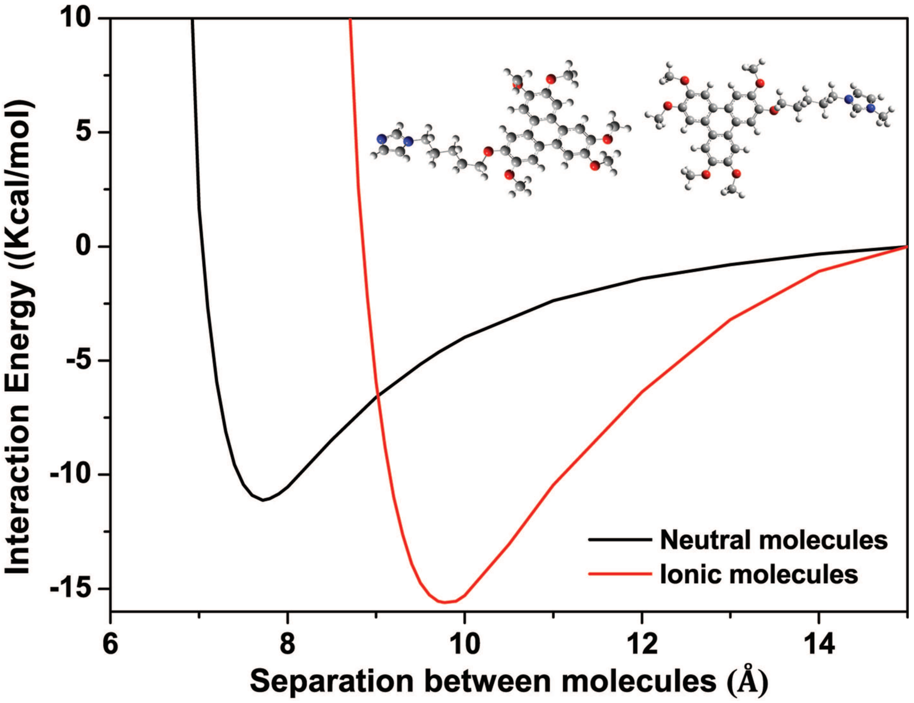

Figure 3.4: Plot showing interaction energy(kcal/mol) as a function of inter planar distance between the two molecules in gaseous phase

angles of vector C1 C2 along with Z-axis. These calculations were done for both neutral and ionic molecules and the results were studied comparatively.

As the barriers in the LB system moves closer to each other, the surface area of water along with the ImTp molecules on its surface reduces. Thus, the concentration of ImTp molecules increases and finally it was observed that the orientation of these molecules tends to shift towards Z-axis. System with the smallest surface area per molecule i.e. 0.5 nm^2/mol is represented by red line and their orientation is highest among all systems. Also the increase in surface area, decreases the ordering of molecules. This can observed from the plot shown in (Figure 3.6). The peak observed for lowest area per molecule is much higher than that of other surface areas per molecule.

For neutral molecules, the highest peak was observed between 40° to 50° for molecules with surface area of 0.5 nm^2/mol whereas the peak observed for highest surface area concentration of 2 nm^2/mol was at 78°. Higher peak denotes uniform orientation of molecules along Z-axis. The most concentrated Ionic ImTp

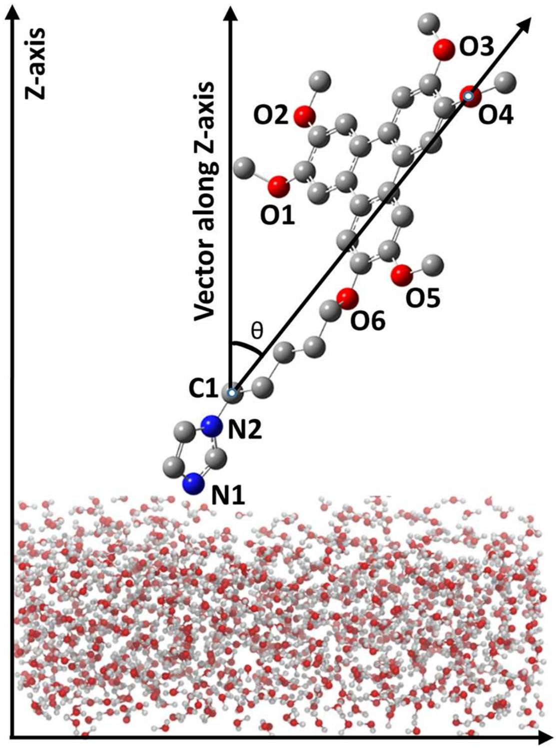

Figure 3.5: showing the vector considered for Z-orientation and various labelled atoms.

molecules showed peak in the range of 45° to 58° whereas the least concentrated in the range of 50° to 75°.

The effect of surface concentration is a much more dominant phenomenon in case of neutral ImTp molecules as these molecules are spread over 30° to 110° whereas ionic molecules were spread just over 45° to 75° only. Thus, we can state that ordering of molecules is much more uniform in ionic molecules than in neutral. Since neutral molecules favour hydrogen bonding between nitrogen and water molecules, they are spread in a long range of angle and have a non-uniform orientation. But the effect of surface concentration is quite high in neutral molecules and is dominating over hydrogen bonding. The increase in surface concentration increases the orientation of these molecules along the Z-axis.

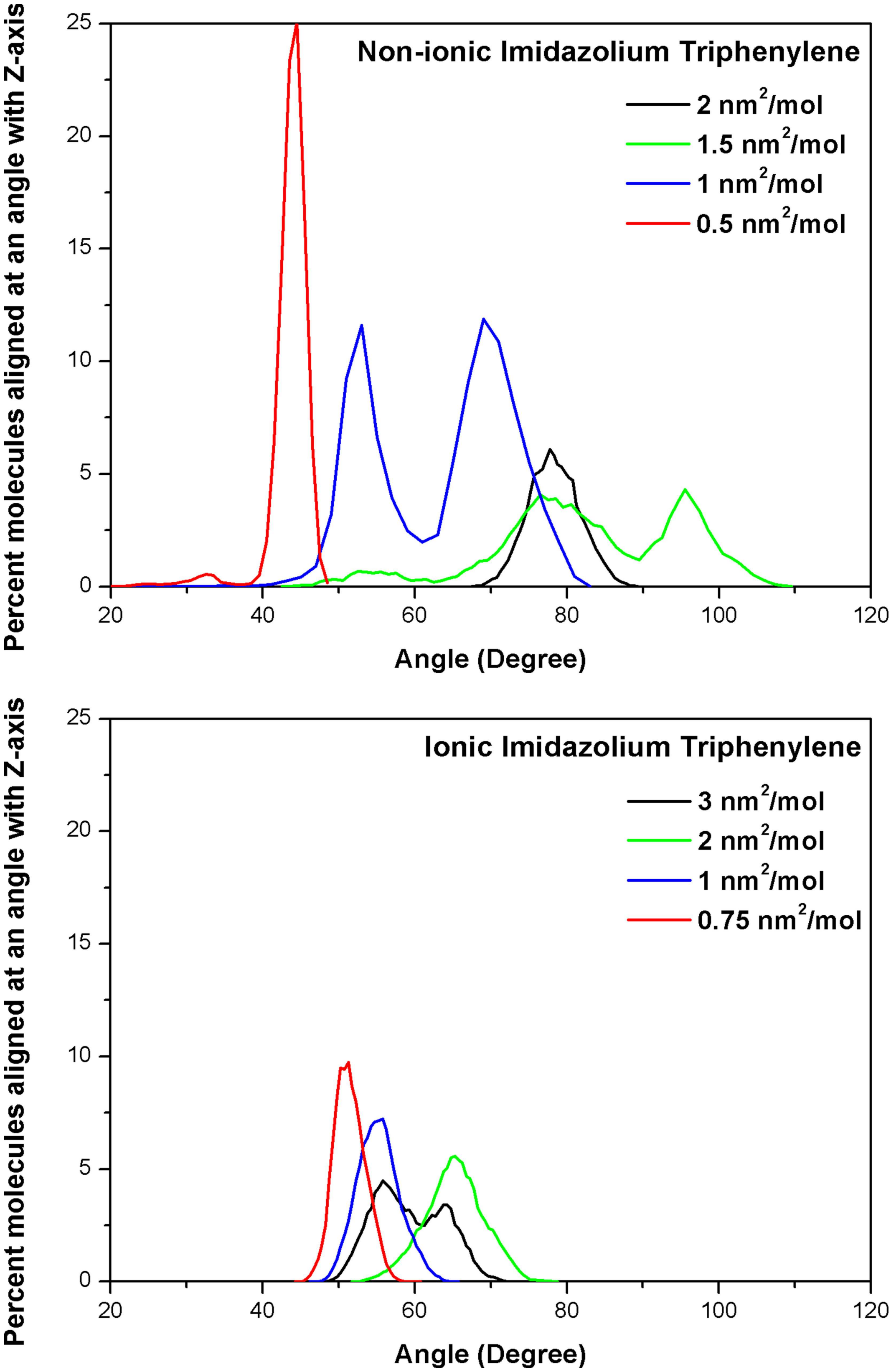

FIGURE 3.6: Percentage orientation of ImTp molecules along Z-axis as function of angle

3.3.3 Z-Density

For computing the average number density of head group and tail group along the z-axis, density utility was used. The head group (N1 N2) and tail group (O6) are shown in figure Figure 3.5. The Z-number density depicts the average number of atoms present at a xy-plane w.r.t z-axis. The Z-number density plot for neutral Im Tp molecules are shown in (Figure 3.7). The probability of finding head group is represented by black curve whereas tail group by red. The area per unit molecule of the systems are in decreasing fashion and is mentioned in the respective plots.

It can be observed from the plot that as the surface area of system decreases, the probability density peaks shift away. The increase in the shift of these two peaks means that ImTp molecule is orienting towards the Z-axis. For large area per molecule the peaks are almost overlapping. But as we reduce the area below 1 nm^2/mol, there is a shift in peak. Hence molecules start orienting themselves along the Z-axis from this point onwards. Also as the surface area per molecule decreases, the probability of finding head and tail group increases which concludes that the arrangement of molecules becomes more ordered with decrease in surface area.

A major factor which distinguishes the arrangement of neutral ImTp molecules from ionic is that they are largely dependent on surface area. The Z-Density plot for ionic molecules is shown in (Figure 3.8) This can stated because of the fact that the Z-density plot for head and tail group for ionic systems are almost overlapping at all surface areas per molecule. But in case of non-ionic system, there was a very small overlap between the head and tail group for surface area concentration of 0.5 nm^2/mol. Average number of hydrogen bonds were calculated in order to understand the surface concentration effect on orientation of ImTp DLC molecules.

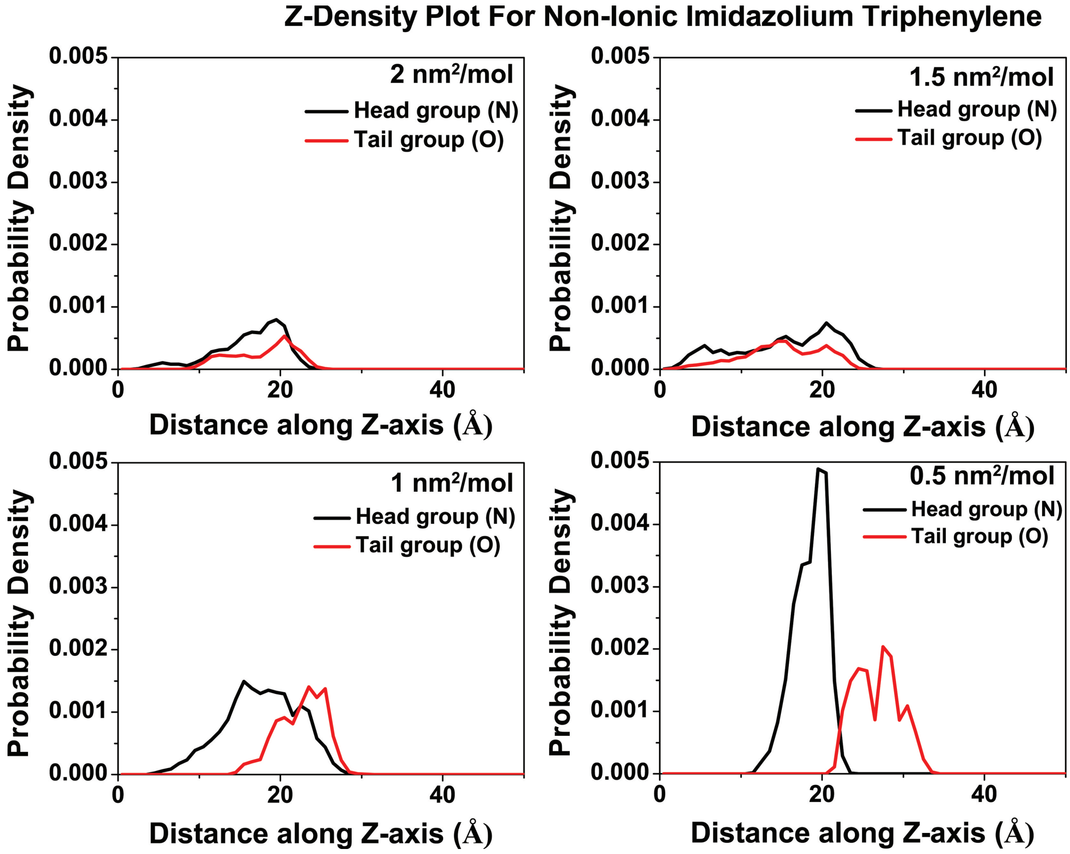

FIGURE 3.7: Probability density plot for neutral ImTp molecules as surface area per molecule varies w.r.t distance along z-axis

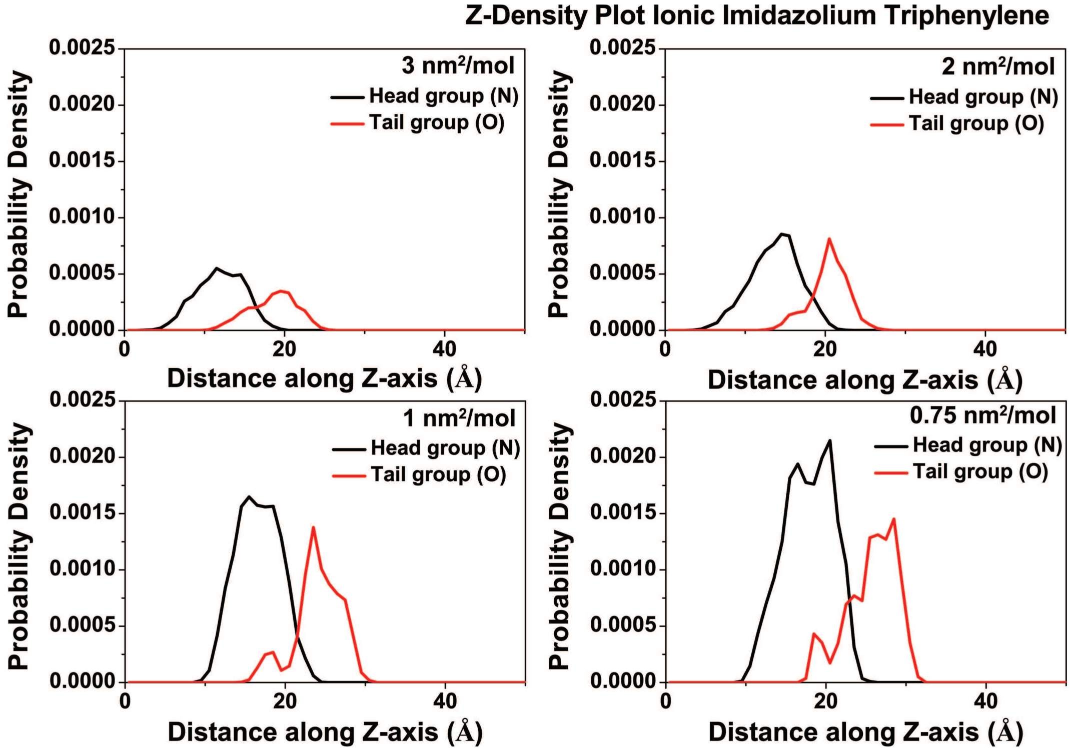

FIGURE 3.8: Probability density plot for ionic ImTp molecules as surface area per molecule varies w.r.t distance along z-axis

3.3.4 Hydrogen Bonding

Since these molecules are on water surface hence hydrogen bonding plays an important role in describing the stability of film. Number of hydrogen bonds were computed based on the cut-off distance and angle between acceptor-hydrogen and hydrogen-acceptor-oxygen respectively. Here the acceptor refers to the atom for which these numbers were calculated and hydrogen and oxygen atoms refers to of water molecule. The conditions for recognising a bond as hydrogen bond was met if the bond length between Acceptor and Oxygen was less than 3.5 Å and bond length between Acceptor and Hydrogen was less than 2.45 Å and the angle subtended by Acceptor and Hydrogen was less than 30°. If and only if all the three conditions mentioned above were fulfilled, it was classified as a H-bond. All the number of hydrogen bonds calculated at each time frame were averaged for all the atoms mentioned in Figure 3.5.

The respective number of hydrogen bonds for neutral ImTp molecules is shown in Table 3.3. From the data it can be observed that average number of hydrogen bonds for Nitrogen atoms were relatively higher than other atoms. Thus, N1 and N2 atoms actively took participation in forming hydrogen bonding with water. This can be a strong reason for face on pi stacking of neutral DLC molecules. Also, due to hydrogen bonding these molecules were spread at different orientation on the surface of water.

Table 3.3: Showing the average number of Hydrogen bond associated with different atoms for neutral ImTp molecules

Area/mol	N1[a]	N2	O1	O2	O3	O4	O5	O6
0.5	0.880	0.4372	0.1818	0.0160	0.0109	0.1327	0.1234	0.2129
1	1.062	0.5509	0.3053	0.2298	0.2582	0.4798	0.3719	0.4278
1.5	0.962	0.4867	0.3248	0.4370	0.4976	0.8120	0.5603	0.4377
2	1.056	0.5427	0.3401	0.3466	0.3719	0.6343	0.4462	0.4857

[a] Atoms are labelled as per Figure 3.5.

Whereas in case of ionic ImTp molecules because of a presence of positive charge on nitrogen atoms hydrogen bonding was rarely possible. The average number of hydrogen bonds for ionic ImTp molecules is shown in Table 3.4. But one of the interesting fact about harder pi stacking is that it reduces the ability to form

Table 3.4: Showing the average number of Hydrogen bond associated with different atoms for ionic Im Tp molecules

Area/mol	N1	N2	O1	O2	O3	O4	O5	O6
0.75	0.002	0.0023	0.1878	0.1867	0.0767	0.0641	0.2224	0.3985
1	0.002	0.0023	0.2328	0.2584	0.1155	0.0684	0.2615	0.3186
2	0.003	0.0024	0.2528	0.2620	0.2378	0.1706	0.3139	0.4696
3	0.003	0.0026	0.3793	0.3966	0.1166	0.0721	0.2435	0.4230

hydrogen bonding[33]. Therefore, ionic ImTp molecules had a better stability which can also be verified from the gas phase energy calculations as ionic molecules were 4.5 kcal/mol more stable.

Thus, we can conclude that in neutral molecules parallel stacking and in ionic counterpart T-shaped stacking was found. The stability of ionic molecules stacked together was higher than that of ionic molecules. This phenomenon was also verified from the experimental observations as the collapse pressure for ionic ImTp molecules was relatively higher than that of neutral ImTp molecules. At low surface concentration the orientation of ionic molecules on water surface was much uniform but as we increased the surface concentration neutral molecules oriented in a better way. Also, hydrogen bonding was actively found in neutral molecules whereas in ionic counterpart, it was rare.

Chapter 4

Device Application and Future Outlook

4.1 Introduction

Most of the semiconductor industry is focused in developing high frequency switching devices. We need high performance switching devices for fast computing, large memory and minimum power loss. Moore's law predicted that every two years the size of integrated chip reduces to half. But we can say that for the past decade it has been saturated and we can not dig much deeper with the present silicon based semiconductor technology.

Resistive switching[34] is one such technique which can be promising in developing high performance switch using the concept of quantized conductance. Resistive switching is a technique in which an atomic scale filament is developed when a bias is applied and it provides a conduction pathway. As the bias is removed this filament breaks and conduction is hampered. The process of forming the filament at atomic scale which provides an atomic contact is known as **formation** whereas the process of breaking up of this atomic contact is termed as **extinction**. This type of quantized conductance is a well known phenomenon and has been reported

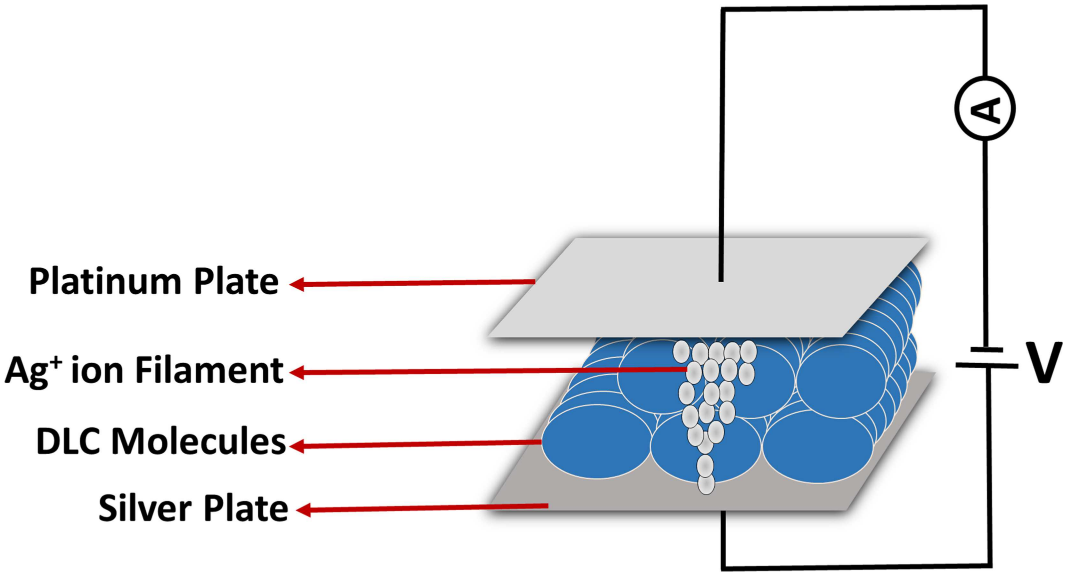

Figure 4.1: Atomic scale filament formation in Metal-DLC-Metal sandwich structure with bias applied externally

in a wide range of materials. In general quantized conductance is expressed as:

$$G_0 = 2e^2/h \tag{4.1}$$

DLC molecules are one of the potential component for such type of devices. A metal-DLC-metal, sandwich layer can be formed to develop such kind of devices as shown in Figure 4.1. A preliminary study has been conducted to study the I-V characteristics of such devices. AFM can be used to mimic such a device as AFM tip serves as a purpose of one of the electrode. Thus, the DLC materials are sandwiched between silver substrate and AFM tip. Platinum or gold coated tip serve for this purpose.

4.2 Experimental Process

A polished silver substrate was deposited with DLC molecule using simple drop cast method. The used DLC molecule sample was synthesized by Dr. S K Pal and his group at IISER Mohali and were provided for experimentation. A single drop of DLC molecule solution in toluene at concentration of 1 mg/mL was cast on silver substrate and was left to dry at room temperature. The sample was placed in Atomic Force Microscope for I-V measurement. The thickness of the molecule was around 40 nm. The I-V characteristics obtained were at room temperature and in ambient atmosphere. AFM tip used for I-V measurement was PPP-CONTSCPt-10. It is a Platinum coated tip with a spring constant of 0.2 N/m and resonant frequency of 23 kHz. For I-V measurement a direct current (DC) voltage sweep was applied. The DC sweep was varied from -10 V to +10 V and was reversed for each cycle. The sweep voltage was fixed to 0.2 V/s with 1500 of total data points. The maximum range of current was of 10 nA and it gets saturated above this limit. The first cycle is called formation cycle and the successive cycles in the same direction are called switching cycles. When a reverse cycle is applied the atomic scale filament breaks down and is known as breaking or extinction cycle. The stability of these filaments are also dependent upon various parameters such as temperature, polarity of bias etc. A stop watch timer was used to measure the time interval between two switching cycles. Studying the time dependence of filament is necessary to understand the filament stability w.r.t to thermal vibration of molecules.

4.3 Result and Discussion

4.3.1 Forming Cycles

To obtain the I-V characteristics for filament formation process, the substrate was biassed using the DC sweep from -10 V to +10 V. The I-V plot is shown in Figure 4.2 for a single DC sweep in both direction of polarity. The red curve is for the increasing polarity from -10 V to +10 V. The formation voltage is at 3.4 V which means that filament is formed at this point making a atomic scale contact between the Silver substrate and AFM tip. When the polarity was reversed i.e, from +10 V to -10 V, the current starts to decay at 1 V and the device turns off completely at 0.5 V. Thus, we can say that breaking of filament takes place at this voltage.

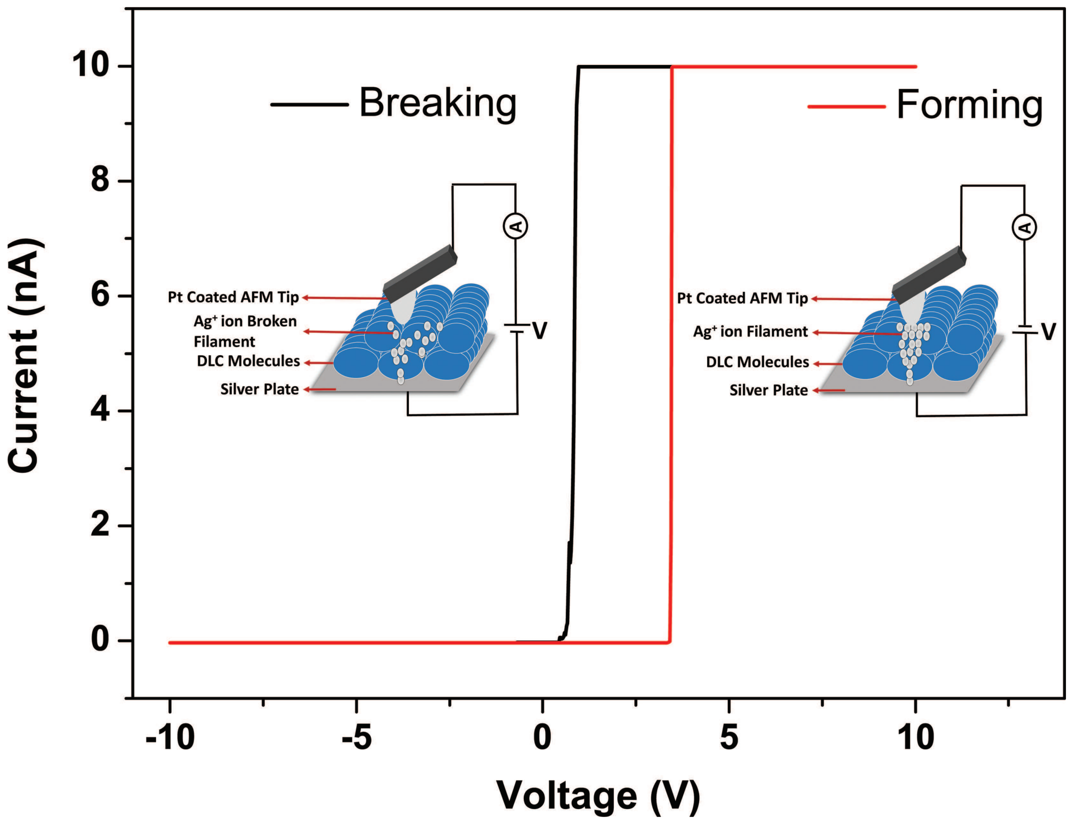

FIGURE 4.2: Forming and Breaking cycles in Atomic Switch device

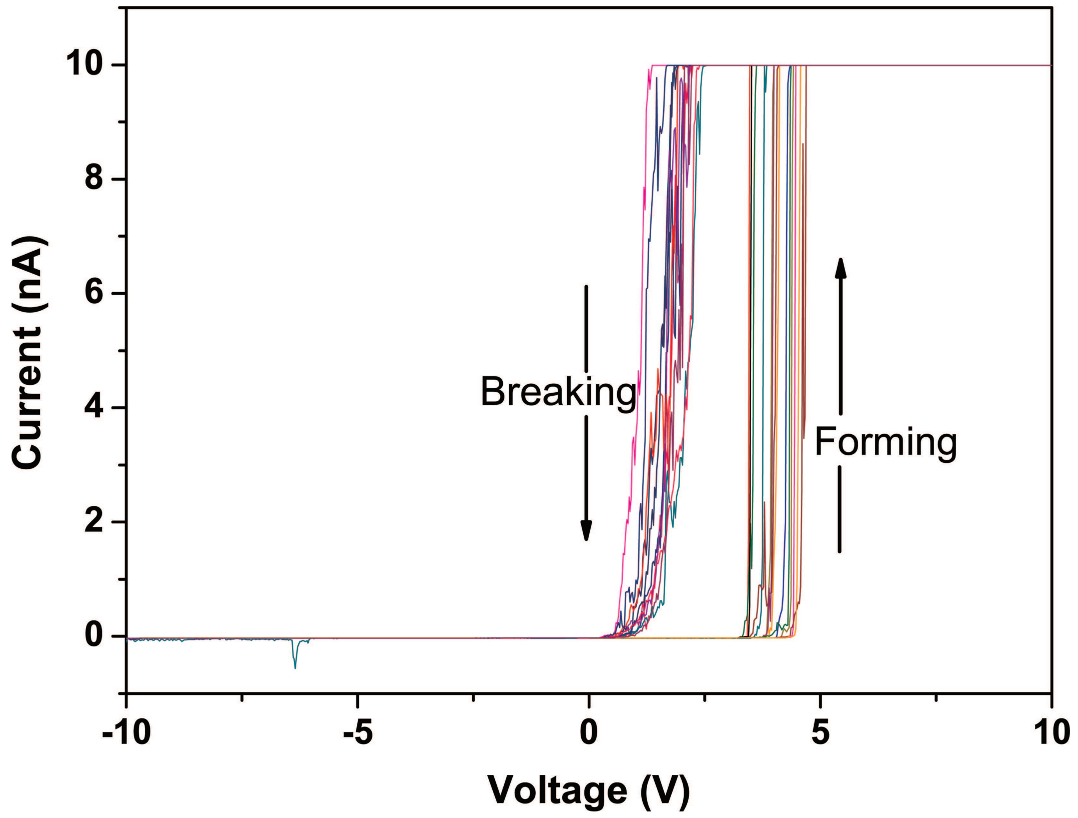

FIGURE 4.3: Forming and Breaking cycles repeated several times

This experiment was repeated several times and the I-V plot is shown in Figure 4.3. From the plot we can conclude that, formation and breaking voltage levels are almost constant and the filament stability is consistent. But one of the major factor is that the device turns off within the positive level of voltage. Hence, the filament is not highly stable and it may dissolve by the motion of ions due to thermal vibration or some other factors.

4.3.2 Switching Cycles

In the similar way to determine the difference between formation voltage and successive switching voltages, I-V characteristics was obtained as shown Figure 4.4. In this I-V characteristic the first DC sweep is represented by black curve. The DC sweep was provided from -10 V to +10 V. The formation voltage is at 5.2 V. The other curves are switching cycles. DC sweep for these cycles was provided from 0 V to +10 V. Hence, the filament was not dissolved in case of switching cycles and was present even before the polarity was applied.

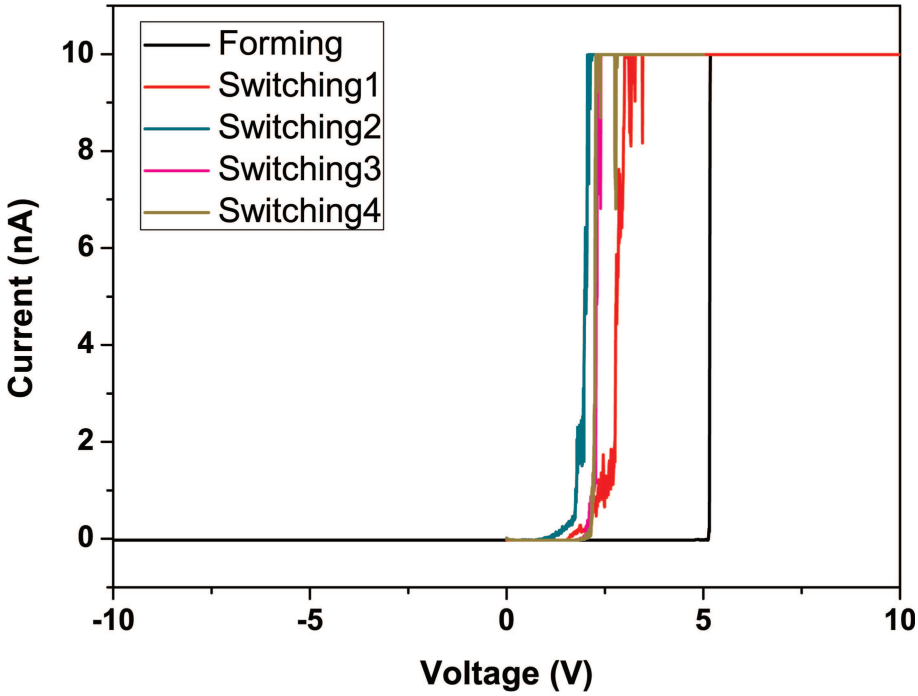

Figure 4.4: IV characteristics for first forming and other switching cycles

It can be seen from the I-V characteristics that the switching voltage is way before the formation voltage and the device starts conducting as the positive bias is applied. The experiment was repeated several times and is shown for four switching cycles just for simplicity of curve. We can conclude that the filament was stable even after removal of polarity and conduction took place from 0 V for the switching cycles.

4.3.3 Effect of Time

To study the effect of time on the filament stability I-V characteristics were obtained after certain time intervals. The filament was left unbiased for this interval of time and a positive DC sweep was provided to test the filament stability. The I-V characteristic as a variation of time is shown in Figure 4.5. The first DC sweep is provided from -10 V to +10 V and is the formation cycle. Afterwards, a time gap of 15 min was given before providing positive DC sweep. The red curve represent the I-V curve after 15 min of filament formation. It can be observed from the plot that the device turns on but not directly from 0 V.

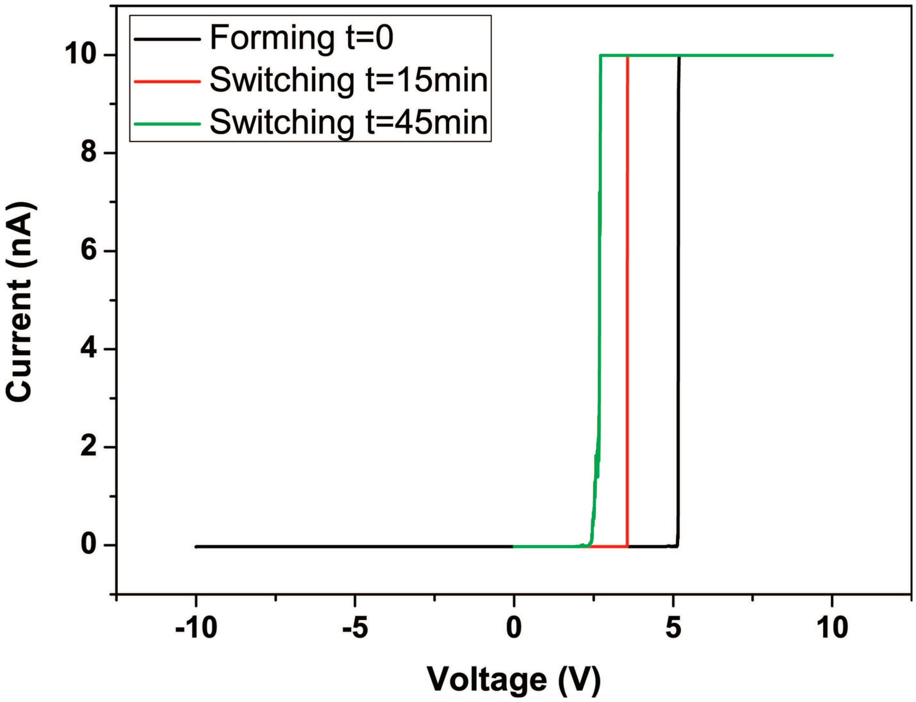

FIGURE 4.5: IV characteristics for forming cycles at different interval of time

Thus, the filament decays as a function of time. The second filament formation takes place at 3.5 V. Again a time interval of 30 min was provided for which the device was unbiased. Green curve represents the I-V characteristics for the switching after 45 min from the first formation cycle. The device turns on at 2.36 V and thus we can say that the filament is not stable w.r.t time.

4.4 Future Outlook

Organic resistive switching devices can be one of the promising field in developing next generation switching devices with high frequency, low on state power loss and high reverse voltage stability. These devices are based on quantized conductance phenomenon and hence by controlling the filament growth, we can control switching of these type of devices. Resistive switching using DLC materials is unprecedented in literature and a large amount of research is still required for commercialising these class of devices. Atomic Switch like devices as shown in Figure 4.1 can be used as organic memristive[35] devices. These devices can be used to store and process large chunk of data and can easily take over silicon integrated chip technology[36]. The high rate of electrical switching and a compact size around 10 nm makes them a viable choice in designing high computation technology.

To understand the supramolecular assembly of DLC molecules on silver substrate, MD simulations and DFT calculations can play a significant role. From some of the preliminary experimental results it has also been discovered that the stability of thin films using DLC molecules along with DNA is increased exponentially. A theoretical understanding on DLC molecules with DNA sample is also important.

With the discovery of DLC molecules a vast avenue of research have been opened in the field of organic devices and it can be a potential candidate in designing organic resistive switching devices.

Bibliography

[1] P. G. de Gennes and J. Prost. *The Physics of Liquid Crystals*. International Series of Monogr. Clarendon Press, 1995. ISBN 9780198517856. URL `https://books.google.co.in/books?id=0Nw-dzWz5agC`.

[2] S. Chandrasekhar, B. K. Sadashiva, and K. A. Suresh. Liquid crystals of disc-like molecules. *Pramana*, 9(5):471–480, Nov 1977. ISSN 0973-7111. doi: 10.1007/BF02846252. URL `https://doi.org/10.1007/BF02846252`.

[3] Hardouin, F. and Levelut, A.M. X-ray study of the reentrant polymorphism n-sa-n-sa in a pure liquid crystal compound. *J. Phys. France*, 41(1):41–46, 1980. doi: 10.1051/jphys:0198000410104100. URL `https://doi.org/10.1051/jphys:0198000410104100`.

[4] Sergey Sergeyev, Wojciech Pisula, and Yves Henri Geerts. Discotic liquid crystals: a new generation of organic semiconductors. *Chem. Soc. Rev.*, 36: 1902–1929, 2007. doi: 10.1039/B417320C. URL `http://dx.doi.org/10.1039/B417320C`.

[5] Sandeep Kumar. Self-organization of disc-like molecules: chemical aspects. *Chem. Soc. Rev.*, 35:83–109, 2006. doi: 10.1039/B506619K. URL `http://dx.doi.org/10.1039/B506619K`.

[6] Yue Zhang, David A. Hanifi, M. Paz Fernndez-Liencres, Liana M. Klivansky, Biwu Ma, Amparo Navarro, and Yi Liu. Understanding electron transport in disk-shaped triphenylene-tris(naphthaleneimidazole)s through structural modification and theoretical investigation. *ACS Applied Materials &*

Interfaces, 9(23):20010–20019, 2017. doi: 10.1021/acsami.7b03795. URL `https://doi.org/10.1021/acsami.7b03795`. PMID: 28534391.

[7] Topolgen Tools. Programs written by gromacs users: Other software. URL `http://www.gromacs.org/Downloads/User_contributions/Other_software,topolgen-1.1.tgz`.

[8] Irving Langmuir. The constitution and fundamental properties of solids and liquids. part i. solids. *Journal of the American Chemical Society*, 38(11): 2221–2295, 1916. doi: 10.1021/ja02268a002. URL `https://doi.org/10.1021/ja02268a002`.

[9] Katharine B. Blodgett. Films built by depositing successive monomolecular layers on a solid surface. *Journal of the American Chemical Society*, 57(6): 1007–1022, 1935. doi: 10.1021/ja01309a011. URL `https://doi.org/10.1021/ja01309a011`.

[10] G. Binnig, H. Rohrer, Ch. Gerber, and E. Weibel. Surface studies by scanning tunneling microscopy. *Phys. Rev. Lett.*, 49:57–61, Jul 1982. doi: 10.1103/PhysRevLett.49.57. URL `https://link.aps.org/doi/10.1103/PhysRevLett.49.57`.

[11] Sandeep Kumar and Santanu Kumar Pal. Synthesis and characterization of novel imidazolium-based ionic discotic liquid crystals with a triphenylene moiety. *Tetrahedron Letters*, 46(15):2607 – 2610, 2005. ISSN 0040-4039. doi: https://doi.org/10.1016/j.tetlet.2005.02.100. URL `http://www.sciencedirect.com/science/article/pii/S0040403905003989`.

[12] Alpana Nayak, K. A. Suresh, Santanu Kumar Pal, and Sandeep Kumar. Films of novel mesogenic molecules at airwater and airsolid interfaces. *The Journal of Physical Chemistry B*, 111(38):11157–11161, 2007. doi: 10.1021/jp073196z. URL `https://doi.org/10.1021/jp073196z`. PMID: 17760436.

[13] Marcus D. Hanwell, Donald E. Curtis, David C. Lonie, Tim Vandermeersch, Eva Zurek, and Geoffrey R. Hutchison. Avogadro: an advanced semantic

chemical editor, visualization, and analysis platform. *Journal of Cheminformatics*, 4(1):17, Aug 2012. ISSN 1758-2946. doi: 10.1186/1758-2946-4-17. URL `https://doi.org/10.1186/1758-2946-4-17`.

[14] Roy Dennington, Todd A. Keith, and John M. Millam. Gaussview Version 6, 2016. Semichem Inc. Shawnee Mission KS.

[15] M. J. Frisch, G. W. Trucks, H. B. Schlegel, G. E. Scuseria, M. A. Robb, J. R. Cheeseman, G. Scalmani, V. Barone, G. A. Petersson, H. Nakatsuji, X. Li, M. Caricato, A. V. Marenich, J. Bloino, B. G. Janesko, R. Gomperts, B. Mennucci, H. P. Hratchian, J. V. Ortiz, A. F. Izmaylov, J. L. Sonnenberg, D. Williams-Young, F. Ding, F. Lipparini, F. Egidi, J. Goings, B. Peng, A. Petrone, T. Henderson, D. Ranasinghe, V. G. Zakrzewski, J. Gao, N. Rega, G. Zheng, W. Liang, M. Hada, M. Ehara, K. Toyota, R. Fukuda, J. Hasegawa, M. Ishida, T. Nakajima, Y. Honda, O. Kitao, H. Nakai, T. Vreven, K. Throssell, J. A. Montgomery, Jr., J. E. Peralta, F. Ogliaro, M. J. Bearpark, J. J. Heyd, E. N. Brothers, K. N. Kudin, V. N. Staroverov, T. A. Keith, R. Kobayashi, J. Normand, K. Raghavachari, A. P. Rendell, J. C. Burant, S. S. Iyengar, J. Tomasi, M. Cossi, J. M. Millam, M. Klene, C. Adamo, R. Cammi, J. W. Ochterski, R. L. Martin, K. Morokuma, O. Farkas, J. B. Foresman, and D. J. Fox. Gaussian16 Revision B.01, 2016. Gaussian Inc. Wallingford CT.

[16] Axel D. Becke. Densityfunctional thermochemistry. iii. the role of exact exchange. *The Journal of Chemical Physics*, 98(7):5648–5652, 1993. doi: 10.1063/1.464913. URL `https://doi.org/10.1063/1.464913`.

[17] Chengteh Lee, Weitao Yang, and Robert G. Parr. Development of the colle-salvetti correlation-energy formula into a functional of the electron density. *Phys. Rev. B*, 37:785–789, Jan 1988. doi: 10.1103/PhysRevB.37.785. URL `https://link.aps.org/doi/10.1103/PhysRevB.37.785`.

[18] S. H. Vosko, L. Wilk, and M. Nusair. Accurate spin-dependent electron liquid correlation energies for local spin density calculations: a critical analysis.

Canadian Journal of Physics, 58(8):1200–1211, 1980. doi: 10.1139/p80-159. URL `https://doi.org/10.1139/p80-159`.

[19] P. J. Stephens, F. J. Devlin, C. F. Chabalowski, and M. J. Frisch. Ab initio calculation of vibrational absorption and circular dichroism spectra using density functional force fields. *The Journal of Physical Chemistry*, 98(45): 11623–11627, 1994. doi: 10.1021/j100096a001. URL `https://doi.org/10.1021/j100096a001`.

[20] H.J.C. Berendsen, D. van der Spoel, and R. van Drunen. Gromacs: A message-passing parallel molecular dynamics implementation. *Computer Physics Communications*, 91(1):43 – 56, 1995. ISSN 0010-4655. doi: https://doi.org/10.1016/0010-4655(95)00042-E. URL `http://www.sciencedirect.com/science/article/pii/001046559500042E`.

[21] William L. Jorgensen and Julian Tirado-Rives. Potential energy functions for atomic-level simulations of water and organic and biomolecular systems. *Proceedings of the National Academy of Sciences*, 102(19):6665–6670, 2005. ISSN 0027-8424. doi: 10.1073/pnas.0408037102. URL `http://www.pnas.org/content/102/19/6665`.

[22] Leela S. Dodda, Jonah Z. Vilseck, Julian Tirado-Rives, and William L. Jorgensen. 1.14*cm1a-lbcc: Localized bond-charge corrected cm1a charges for condensed-phase simulations. *The Journal of Physical Chemistry B*, 121(15): 3864–3870, 2017. doi: 10.1021/acs.jpcb.7b00272. URL `https://doi.org/10.1021/acs.jpcb.7b00272`. PMID: 28224794.

[23] Leela S. Dodda, Israel Cabeza de Vaca, Julian Tirado-Rives, and William L. Jorgensen. Ligpargen web server: an automatic opls-aa parameter generator for organic ligands. *Nucleic Acids Research*, 45(W1):W331–W336, 2017. doi: 10.1093/nar/gkx312. URL `+http://dx.doi.org/10.1093/nar/gkx312`.

[24] Pekka Mark and Lennart Nilsson. Structure and dynamics of the tip3p, spc, and spc/e water models at 298 k. *The Journal of Physical Chemistry A*, 105

(43):9954–9960, 2001. doi: 10.1021/jp003020w. URL `https://doi.org/10.1021/jp003020w`.

[25] Kasper P. Jensen and William L. Jorgensen. Halide, ammonium, and alkali metal ion parameters for modeling aqueous solutions. *Journal of Chemical Theory and Computation*, 2(6):1499–1509, 2006. doi: 10.1021/ct600252r. URL `https://doi.org/10.1021/ct600252r`. PMID: 26627020.

[26] Berk Hess, Henk Bekker, Herman J.C. Berendsen, and Johannes G.E.M. Fraaije. Lincs: A linear constraint solver for molecular simulations. *J. Comput. Chem*, 18:18–1463, 1997.

[27] Tom Darden, Darrin York, and Lee Pedersen. Particle mesh ewald: An nlog(n) method for ewald sums in large systems. *The Journal of Chemical Physics*, 98(12):10089–10092, 1993. doi: 10.1063/1.464397. URL `https://doi.org/10.1063/1.464397`.

[28] Ulrich Essmann, Lalith Perera, Max L. Berkowitz, Tom Darden, Hsing Lee, and Lee G. Pedersen. A smooth particle mesh ewald method. *The Journal of Chemical Physics*, 103(19):8577–8593, 1995. doi: 10.1063/1.470117. URL `https://doi.org/10.1063/1.470117`.

[29] Erik Lindahl, Berk Hess, and David van der Spoel. Gromacs 3.0: a package for molecular simulation and trajectory analysis. *Molecular modeling annual*, 7(8):306–317, Aug 2001. ISSN 0948-5023. doi: 10.1007/s008940100045. URL `https://doi.org/10.1007/s008940100045`.

[30] William Humphrey, Andrew Dalke, and Klaus Schulten. VMD – Visual Molecular Dynamics. *Journal of Molecular Graphics*, 14:33–38, 1996.

[31] John Stone. *An Efficient Library for Parallel Ray Tracing and Animation.* Master's thesis, Computer Science Department, University of Missouri-Rolla, April 1998.

[32] Toni Smith, Lyudmila V. Slipchenko, and Mark S. Gordon*. Modeling interactions with the effective fragment potential method: The benzene dimer

and substituents. *The Journal of Physical Chemistry A*, 112(23):5286–5294, 2008. doi: 10.1021/jp800107z. URL `https://doi.org/10.1021/jp800107z`. PMID: 18476681.

[33] Pierre Mignon, Stefan Loverix, Jan Steyaert, and Paul Geerlings. Influence of the interaction on the hydrogen bonding capacity of stacked dna/rna bases. *Nucleic Acids Research*, 33(6):1779–1789, 2005. doi: 10.1093/nar/gki317. URL `http://dx.doi.org/10.1093/nar/gki317`.

[34] Takami Hino, Tsuyoshi Hasegawa, Kazuya Terabe, Tohru Tsuruoka, Alpana Nayak, Takeo Ohno, and Masakazu Aono. Atomic switches: atomic-movement-controlled nanodevices for new types of computing. *Science and Technology of Advanced Materials*, 12(1):013003, 2011. URL `http://stacks.iop.org/1468-6996/12/i=1/a=013003`.

[35] Leon Chua. If its pinched its a memristor. *Semiconductor Science and Technology*, 29(10):104001, 2014. URL `http://stacks.iop.org/0268-1242/29/i=10/a=104001`.

[36] J. Joshua Yang, Dmitri B. Strukov, and Duncan R. Stewart. Memristive devices for computing. *Nature Nanotechnology*, 8:13 EP –, Dec 2012. URL `http://dx.doi.org/10.1038/nnano.2012.240`. Review Article.